Neuron

Article

Top-down control of exogenous attentional selection is mediated by beta coherence in prefrontal cortex

Graphical abstract

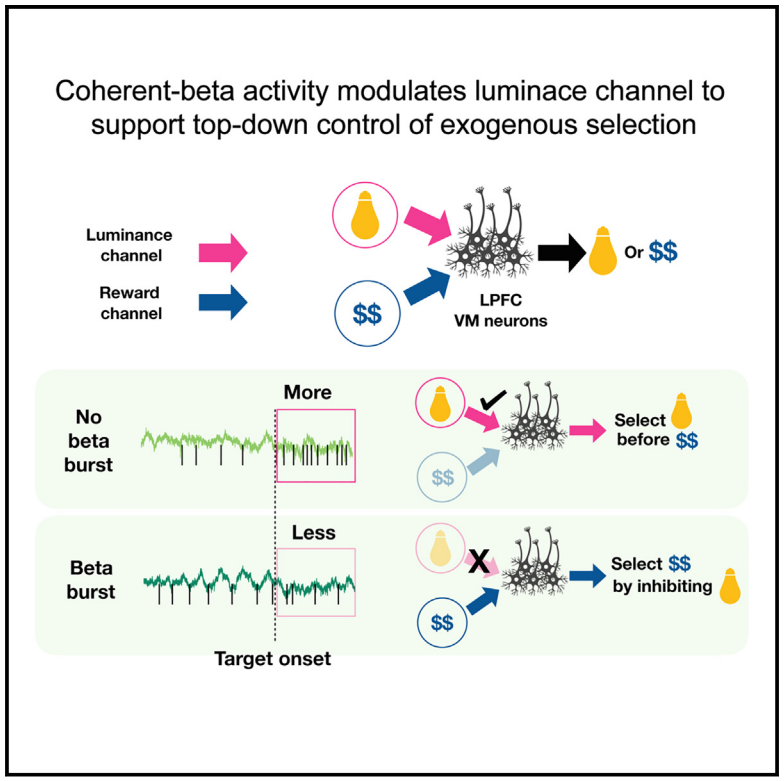

Authors

Agrita Dubey, David A. Markowitz, Bijan Pesaran

Correspondence

pesaran@upenn.edu

In brief

Dubey et al. demonstrate inhibitory network mechanisms of top-down control of attentional selection in the prefrontal cortex. A specific neuronal-response class—visual-movement neurons—encodes exogenous and endogenous selection. Coherent beta activity selectively suppresses sensory information flow in these neurons to favor endogenous selection during conflict.

Highlights

- Visual-movement neurons encode exogenous and endogenous attentional selection
- Coherent beta activity selectively modulates mechanisms of exogenous selection
- Beta activity suppresses exo-selection when in conflict with endo-selection
- Beta-activity-mediated mechanisms selectively inhibit visual-movement neurons

Dubey et al., 2023, Neuron *111*, 1–14
October 18, 2023
https://doi.org/10.1016/j.neuron.2023.06.025

CellPress

Neuron

CellPress

Article

Top-down control of exogenous attentional selection is mediated by beta coherence in prefrontal cortex

Agrita Dubey,[1,3] David A. Markowitz,[1] and Bijan Pesaran[1,2,3,4,*]
[1]Center for Neural Science, New York University, New York, NY 10003, USA
[2]Departments of Neurosurgery, Neuroscience, and Bioengineering, University of Pennsylvania, Philadelphia, PA 19104, USA
[3]Current address: Department of Neurosurgery, University of Pennsylvania, Philadelphia, PA 19104, USA
[4]Lead contact
*Correspondence: pesaran@upenn.edu
https://doi.org/10.1016/j.neuron.2023.06.025

SUMMARY

Salience-driven exogenous and goal-driven endogenous attentional selection are two distinct forms of attention that guide selection of task-irrelevant and task-relevant targets in primates. Top-down attentional control mechanisms enable selection of the task-relevant target by limiting the influence of sensory information. Although the lateral prefrontal cortex (LPFC) is known to mediate top-down control, the neuronal mechanisms of top-down control of attentional selection are poorly understood. Here, we trained two rhesus monkeys on a two-target, free-choice luminance-reward selection task. We demonstrate that visual-movement (VM) neurons and nonvisual neurons or movement neurons encode exogenous and endogenous selection. We then show that coherent beta activity selectively modulates mechanisms of exogenous selection specifically during conflict and consequently may support top-down control. These results reveal the VM-neuron-specific network mechanisms of attentional selection and suggest a functional role for beta-frequency coherent neural dynamics in the modulation of sensory communication channels for the top-down control of attentional selection.

INTRODUCTION

In primates, selection of task-relevant targets is guided by goal-driven ("top-down") endogenous attentional processes, whereas selection of task-irrelevant distractors is guided by salience-driven exogenous ("bottom-up") attentional processes.[1–6] Exogenous selection is fast and occurs earlier in time, whereas endogenous selection is slow and occurs later in time.[2,7–9] Therefore, trial-by-trial flexible selection behavior depends on the dynamic interplay between exogenous and endogenous attentional mechanisms.[2,7,9,10] However, how attentional selection is controlled when exogenous and endogenous attentional mechanisms are in conflict remains unclear. How is the task-relevant target selected when in conflict with the salient target?

Endogenous attentional selection relies on a top-down control process that enables the selection of task-relevant targets by limiting the influences of automatic-salience selection.[11–13] Neural mechanisms that support top-down control are distributed throughout the fronto-parietal regions and rely heavily on the lateral prefrontal cortex (LPFC)[9,13–18] as evident from lesion experiments.[19–23] Thus, LPFC-mediated top-down control mechanisms may support selection of the task-relevant target when in conflict with the task-irrelevant salient target.

Information flow about task-relevant and -irrelevant targets during conflict must be mediated by multiregional communication and, specifically, competition between convergent information streams. Since exogenous attentional selection is fast and processes sensory streams of information while endogenous attentional selection is slow and processes information about goals, each attentional process operates across distinct neural pathways, i.e., communication channels (Figure 1A). Consequently, selective filtering of information flow across sensory and reward-based communication channels may support the top-down control of attentional selection.

Neuronal coherence, measured by local field potential (LFP) activity in specific frequency bands, reveals the correlations in the timing of neural activity across populations of neurons[25] and is generally interpreted in terms of multiregional communication.[26–28] Many studies highlight the importance of multiregional communication and neuronal coherence to attentional selection. Attentional selection involves interactions between populations of LPFC neurons.[29,30] In the LPFC, cue-triggered LFP activity in the beta-frequency (15–35 Hz) band reflects exogenous selection.[9,30] Beta-frequency activity after the cue also reflects endogenous selection and suppression of sensory information during working memory and attention tasks.[31–37] This suggests that

Please cite this article in press as: Dubey et al., Top-down control of exogenous attentional selection is mediated by beta coherence in prefrontal cortex, Neuron (2023), https://doi.org/10.1016/j.neuron.2023.06.025

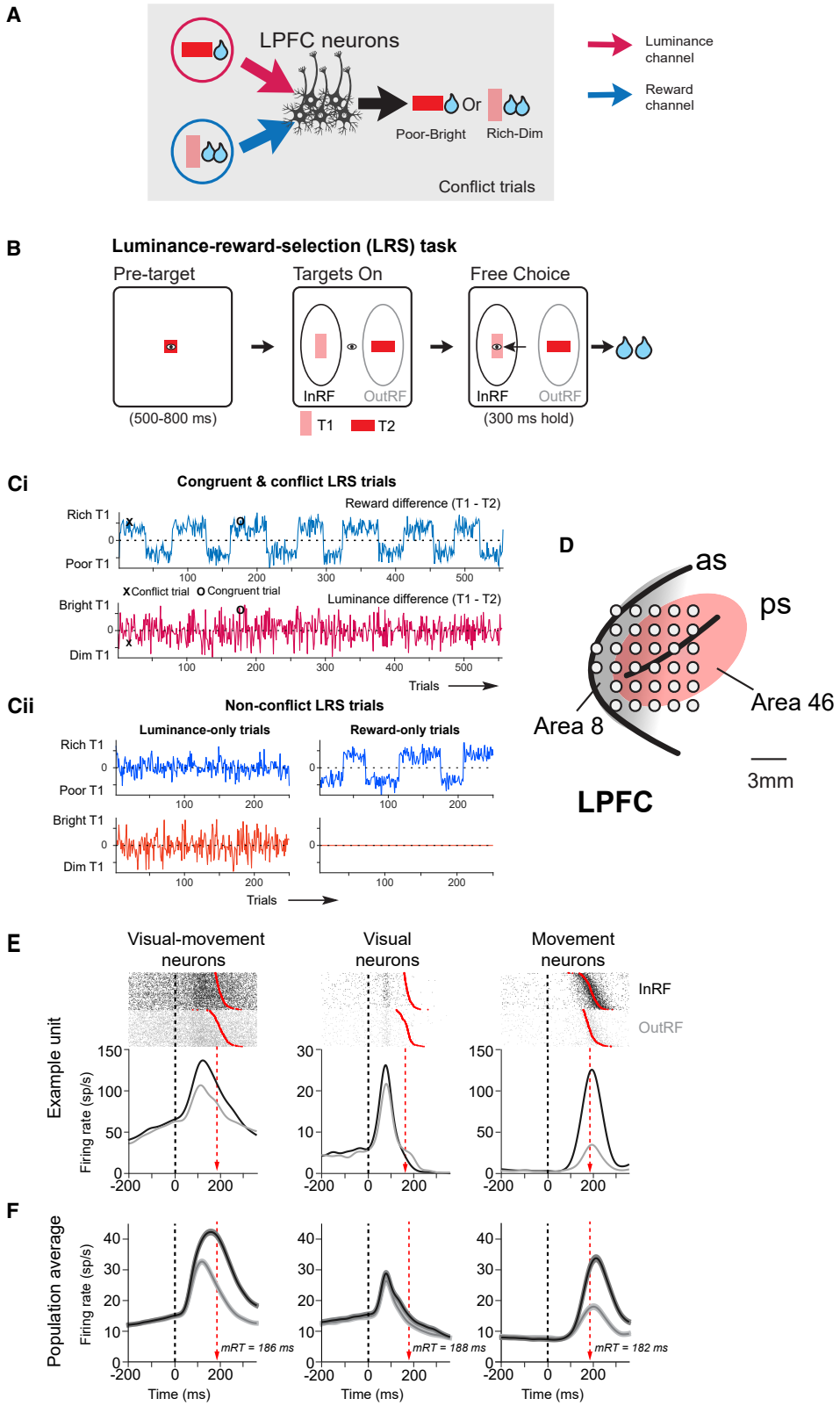

(legend on next page)

Please cite this article in press as: Dubey et al., Top-down control of exogenous attentional selection is mediated by beta coherence in prefrontal cortex, Neuron (2023), https://doi.org/10.1016/j.neuron.2023.06.025

beta-frequency neuronal coherence may support top-down control and the trial-by-trial interplay between endogenous and exogenous attentional selection during conflict. However, prior work has not dissociated endogenous and exogenous selection during conflict to understand how beta-frequency coherence biases information flow across communication channels to guide attentional selection. Whether beta frequency neural coherence acts on communication channels carrying salience-driven or goal-directed information is not known.

Here, we test the neural mechanisms of top-down control of attentional selection and the role of beta-frequency neuronal coherence.

RESULTS

We trained two rhesus macaque monkeys (*Macaca mulatta*) to perform a luminance-reward-selection (LRS) task (Figure 1B; STAR Methods). The LRS task dissociates exogenous and endogenous attentional selection by independently manipulating reward and luminance (Figure 1Ci) to yield either congruent or conflict trials. On congruent trials, luminance and reward value were both high for one target (Rich-Bright) and low for the other (Poor-Dim). On conflict trials, one target was Rich-Dim, while the other was Poor-Bright (Figure 1Ci). The LRS task also featured luminance-only trials with similar relative target reward values and reward-only trials with similar relative target luminance values (Figure 1Cii).

We recorded neural activity from 32 electrodes in the LPFC during LRS task performance (Figure 1D, monkey 1 (M1): n = 39 sessions; monkey 2 (M2): n = 42 sessions), yielding 409 task-responsive single units (M1: 179; M2: 230 neurons). We also recorded the activity of each neuron during a single-target oculomotor delayed response (ODR) task. Spiking activity increased in a spatially selective manner during the ODR trials.[38] Of 409 neurons, 261 neurons were ODR-task responsive with an excitatory response field (64%). Most neurons showed elevated firing activity following target onset and the saccadic response, which we term visual-movement (VM) neurons (n = 139, 53%; Figure S1A). Other neurons increased firing after target onset alone, termed visual neurons (n = 57, 22%; (Figure S1B), or around the saccade and not target onset, termed movement neurons (n = 65, 25%; Figure S1C).

To further analyze the LPFC neuronal population dynamics, we performed a principal-component analysis of activity during the luminance-only trials, which revealed visual and movement modes that explained ~75% firing variability (Figure S1D). We projected the firing rate activity of each group of neurons onto the visual and movement modes (Figures S1F and S1G). While VM neurons showed activity for both visual and movement modes, visual neurons showed activity mainly for the second mode. Movement neurons showed activity mainly for the movement mode and not for the visual mode.

LPFC neurons involved in attentional selection should fire more spikes on trials when the target in the response field (RF) is chosen (InRF) compared with trials when the target outside the RF is chosen (OutRF); see Figures 1E and 1F for LRS task and Figures S1H and S1I for luminance-only and reward-only trials. VM neurons responded significantly more on InRF trials compared with OutRF trials (LRS, $p = 4.2 \times 10^{-3}$; luminance only, $p = 5.8 \times 10^{-4}$; reward only: $p = 4.5 \times 10^{-3}$; rank-sum, 50–200 ms). Movement neurons also responded significantly more during movement on InRF trials compared with OutRF trials, but not immediately after target onset (LRS, $p = 5.7 \times 10^{-5}$; luminance only, $p = 1.1 \times 10^{-3}$; reward only: $p = 3.8 \times 10^{-5}$; rank-sum, 150–250 ms). Visual neurons responded similarly for InRF and OutRF trials (LRS, p = 0.61; rank-sum, 0–100 ms). Visual neurons fired similarly for InRF and OutRF trials on reward-only trials but responded significantly more on InRF, luminance-only trials (luminance only, p = 0.03; reward only, p = 0.62; rank-sum, 0–100 ms). Visual neuron responses are not necessarily due to attention because they are only selective on luminance-only non-conflict trials. These results show that VM neurons play a more direct role in attentional selection, and visual and movement neurons do not.

Visual movement neuron spiking reflects attentional selection

Conflict trials may reveal endogenous, reward-driven selection or exogenous, stimulus-driven selection (Figure 2A). We specifically predicted that reaction time (RT) should be longer on conflict trials when endogenous selection is expressed and the Rich-Dim target (and not the Poor-Bright target) is chosen (i.e., endo-conflict trials) compared with conflict trials when exogenous selection is expressed and the Poor-Bright target is chosen (i.e., exo-conflict trials). RTs were significantly greater for endo-conflict trials compared with exo-conflict trials (M1: endo-conflict RT = 191 ± 29 ms, exo-conflict RT = 169 ± 26 ms, $p = 5.3 \times 10^{-26}$; M2: endo-conflict RT = 192 ± 28 ms, exo-conflict RT = 185 ± 36 ms; $p = 8.2 \times 10^{-21}$; rank-sum, mean ± SEM). Consequently, conflict

Figure 1. Experimental design

(A) Attentional selection involves filtering information flow across communication channels. The luminance channel communicates the task-irrelevant sensory information. The reward channel communicates task-relevant goal information. During conflict, the luminance and reward communication channels compete to guide exogenous or endogenous selection. The top-down control may support exogenous or endogenous selection by filtering either or both of the luminance and reward channels.

(B) Luminance-reward selection (LRS) task events.

(Ci and Cii) (Ci) Congruent and conflict LRS trials. Mean value of reward associated with each target is varied in blocks of 40–70 trials (top). Luminance value associated with each target is randomly selected on each trial (bottom). (Cii) Same as (Ci) except for luminance-only (left) and reward-only (right) trials.

(D) Neural recording locations (white dots). Areas 8 and 46.[24] *as*, arcuate sulcus; *ps*, principal sulcus.

(E) Spike rasters and peristimulus time histogram (PSTH) for a sample visual-movement (VM), visual, and movement neuron for congruent and conflict LRS trials aligned to target presentation. Saccade onset (red dots). Target onset (dotted lines).

(F) PSTH for VM (n = 139, left), visual (n = 57, middle) and movement (n = 65, right) neurons on congruent and conflict LRS trials when target selection was InRF and OutRF. The SEM of firing rates (shaded); average reaction time (RT) (red arrows).

Please cite this article in press as: Dubey et al., Top-down control of exogenous attentional selection is mediated by beta coherence in prefrontal cortex, Neuron (2023), https://doi.org/10.1016/j.neuron.2023.06.025

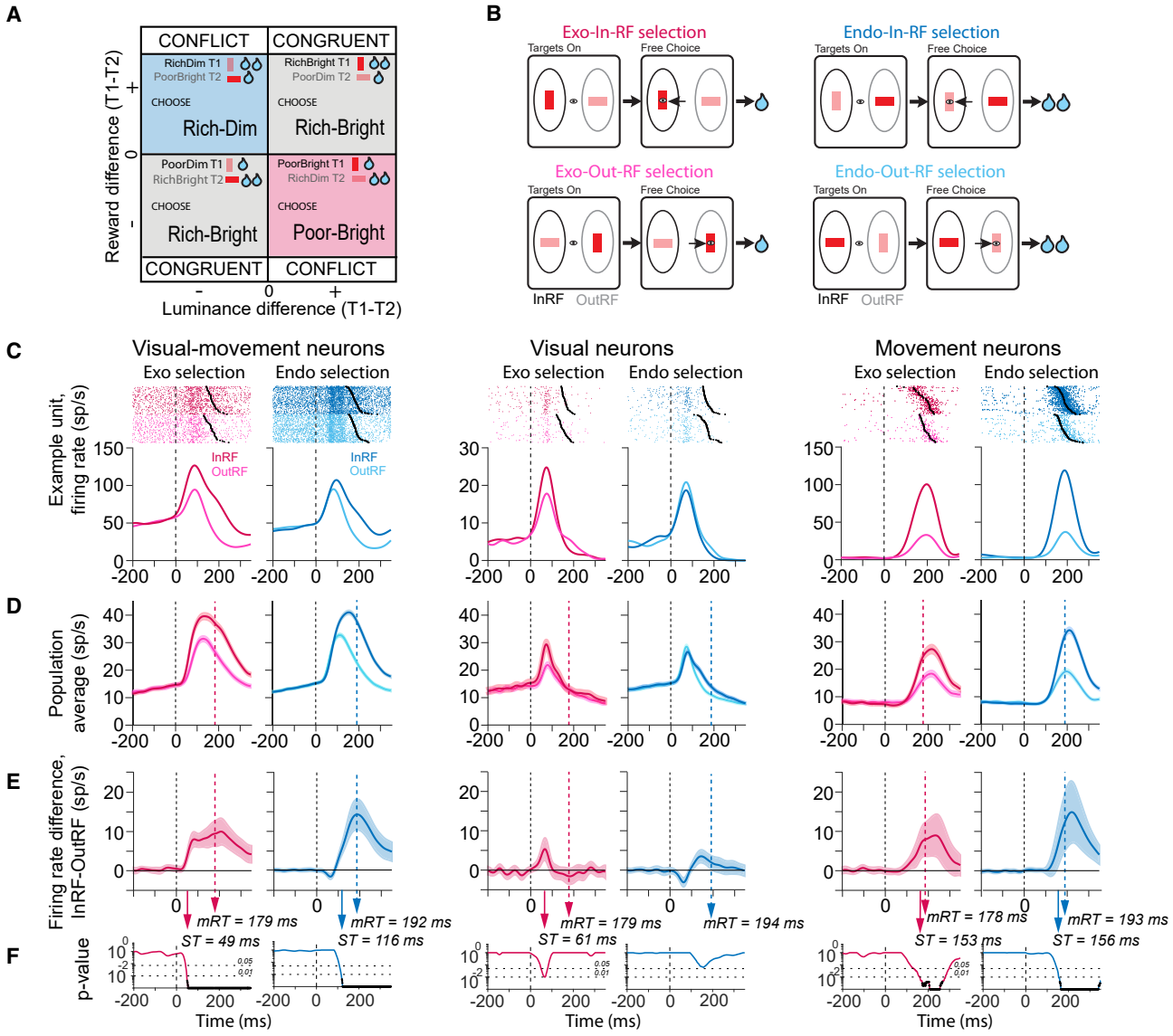

Figure 2. Visual-movement (VM) neurons reflect exogenous and endogenous attentional selection

(A) On congruent trials, luminance and reward value is high for one target (Rich-Bright) and low for other target (Poor-Dim). When both luminance and reward drive are in congruent, they both favored the selection of the Rich-Bright target. On conflict trials, one target has high-reward and low-luminance Rich-Dim while the other has low-reward and high-luminance Poor-Bright. When luminance and reward drive are in conflict, luminance driven choices result in exogenous (exo-) selection of the Poor-Bright target and reward driven choices result in endogenous (endo-) selection of the Rich-Dim target.

(B) Schematic. On exo-InRF trials the selected Poor-Bright target is in the RF while on exo-OutRF trials the selected Poor-Bright target is out of the RF. On endo-InRF trials the selected Rich-Dim target is in the RF while on endo-OutRF trials the selected Rich-Dim target is out of the RF.

(C) Spike raster and peri-stimulus time histogram (PSTH) for exo- and endo- selection of an example visual-movement, visual, and movement neuron on conflict trials shown aligned to the target presentation. Saccade RT (black dots); target onset (dotted line).

(D) PSTH for VM, visual and movement neurons on exo-InRF, exo-OutRF, endo-InRF and endo-OutRF conflict trials. The SEM of firing rates is shaded.

(E) Firing rate difference for selection into and out of the RF for three groups of neurons on conflict trials (top). Mean ± SEM.

(F) Permutation test p values against a null hypothesis that there is no difference in InRF and OutRF firing rates (bottom). False discovery rate (FDR) corrected p values for alpha = 0.01 (black). Arrow: selection time (ST) when first time separation becomes significant (VM: exo ST = 49 ms, endo ST = 116 ms; visual: exo ST = 61 ms; movement: exo ST = 153 ms, endo ST = 156 ms). Average RT for exogenous and endogenous selection trials (dotted lines).

trials revealed whether endogenous selection or exogenous selection was expressed trial-by-trial.

Behavioral choice variations with RT also revealed exogenous and endogenous selection. On conflict trials, shorter RTs reflected exogenous selection, whereas longer RTs reflected endogenous selection (Figures S2A–S2D). On luminance-only trials, shorter RTs reflected exogenous selection and bright-target choice probability approached chance for longer RTs.

On reward-only trials, longer RTs reflected endogenously driven selection, and rich target choice probability approached chance for shorter RTs. Therefore, only conflict trials reveal exogenous and endogenous selection.

We next investigated the underlying neural mechanisms. On exo-conflict trials when the Poor-Bright target is selected and the target is in the RF, exo-InRF trials, neuronal firing should differ from exo-conflict trials when the Poor-Bright target is selected and the target is out of the RF, exo-OutRF trials (Figure 2B). Firing supporting endogenous selection on endo-conflict trials when the Rich-Dim target in the RF is selected, endo-InRF trials, should differ from firing on endo-conflict trials when the Rich-Dim target out of the RF is selected, i.e., endo-OutRF trials (Figure 2B). Since exogenous selection occurs earlier than endogenous selection, neuronal selectivity on exo-conflict trials should occur before endo-conflict trials.

Consistent with its role in attentional selection during conflict, VM neuron selectivity on exo-conflict trials occurred before endo-conflict trials (see, for example, Figure 2C). VM neurons responded more when the InRF target was selected compared with when the OutRF target was selected for both exo-conflict trials and endo-conflict trials. Interestingly, VM neuron firing on InRF trials differed from OutRF trials substantially earlier on exo-conflict trials compared with endo-conflict trials. After the target onset, VM neuron firing rate during exogenous selection separated ~50 ms earlier than during endogenous selection (exo-selection time [ST] = 49 ms, endo-ST = 116 ms) (Figures 2D, 2E, S2E, and S2F). Therefore, VM neurons process both exogenous and endogenous selection during conflict.

VM neuron firing for InRF selection of Poor-Bright target was driven by exogenous attention and was not simply due to physical brightness of the target (Figures S2G and S2H). On luminance-only trials, VM neurons responded more when the bright-target was selected rapidly compared with when the bright-target was selected more slowly (Figure S2G, InRF). Thus, exogenous attention and not physical brightness drives firing.

The firing rates of visual neurons for InRF and OutRF conditions significantly differed on exo-conflict but not on endo-conflict trials ($p < 0.01$, permutation; exo-ST = 61 ms, Figure 2E). Consequently, visual neuron activity likely reflects exogenous selection alone and not conflict with endogenous selection. Movement neurons, however, showed elevated responses on InRF trials compared with OutRF trials for both exo-conflict and endo-conflict trials (Figure 2E). But movement neuron firing rates for two conditions separated at a similar time after the target onset ($p < 0.01$, permutation; exo-ST = 153 ms, endo-ST = 156 ms, Figure S2E). Hence movement neuron activity does not reflect conflict and likely reflects subsequent response preparation and movement. Therefore, only VM neuron firing reflects attentional dynamics during conflict.

LPFC neuron spiking activity contains beta-frequency bursts

We investigated the role of neuronal coherence in LPFC in the control of exogenous and endogenous selection. In the pre-target period, LFP activity on individual electrodes displayed clear bursts of beta-frequency activity (15–30 Hz), which we term beta bursts (Figure 3A). Pre-target beta bursts were clearly and reliably visible in LFP activity on individual trials. When present, beta bursts tended to occur in the pre-target period, not after the target onset, and typically occurred for several hundred milliseconds.

For each trial, we estimated the amplitude of pre-target beta bursts at a single site from 200 ms before target onset until target onset, a duration long enough to sample several cycles of activity at the beta frequency. Beta-burst amplitude varied significantly from trial to trial (for example, see Figure 3B). Across the population, beta bursts were reliably present across LPFC recording locations in each animal (M1: 1,108/1,152 sites; M2: 1,299/1,344 sites; 96% of electrodes, $p < 0.05$ permutation). We grouped the trials with the highest ~33% and lowest ~33% beta burst activity to yield high-beta (HB) trials and low-beta (LB) trials.

We first sought to assess whether beta bursts in LFP activity could reflect a local source in LPFC. To help answer this question, we looked for evidence of coherent activity in the spiking activity of 409 single units in LPFC (M1: n = 179; M2: n = 230) by correlating spiking with nearby LFP activity (within approximately 1.5 mm) using spike-field coherence (SFC) (Figure 3C). During the pre-target period, of the 409 neurons, 176 neurons significantly fired spikes at times predicted by nearby LFP activity in the beta-frequency range (15–35 Hz) ($p < 0.05$, cluster-corrected, permutation; M1: n = 59 and M2: n = 117, Figure S3A). This suggests that beta burst LFP activity involves LPFC neuron firing and is not simply due to activity propagating from other regions that do not necessarily involve LPFC neuron firing. SFC amplitude in LPFC was greatest for activity in the beta-frequency range, compared with frequencies greater than 35 Hz. The number of LPFC neurons that fired coherently in the gamma frequency range (40–70 Hz) was not significant (< 5%, Figure S3B).

Trial-to-trial variability in beta burst amplitude may reflect trial-to-trial changes in the timing of spiking activity across the population of LPFC neurons. If so, spiking during HB trials should display greater coherence than spiking during LB trials. The dependence of neural coherence on beta burst events should specifically be observed in the neurons that participate in the coherent activity. Neurons that do not participate, firing spikes at times that cannot be predicted by beta-frequency neural activity, should not show differences in coherence with beta burst events. To test this, we estimated SFC immediately before target onset separately for the HB and LB trials for coherent and not-coherent neurons (Figures 3D, 3E, and S3C–S3E). Consistent with a strong relationship between spiking and beta burst events, SFC was significantly stronger during HB trials than LB trials for coherent neurons ($p = 9.3 \times 10^{-27}$ rank-sum). The change in coherence for between high and low beta trials was smaller, if not absent, for noncoherent neurons ($p = 0.1$, rank-sum), with the caveat that the lack of an effect in the population of noncoherent neurons may be a flooring effect. While the presence of SFC in coherent neurons may not be due to HB versus LB, the increase in SFC for coherent neurons between HB and LB could be due to higher power in HB. These results demonstrate that when high-amplitude beta bursts occur during the pre-target period, they reflect increased coherent spiking in LPFC neurons.

Please cite this article in press as: Dubey et al., Top-down control of exogenous attentional selection is mediated by beta coherence in prefrontal cortex, Neuron (2023), https://doi.org/10.1016/j.neuron.2023.06.025

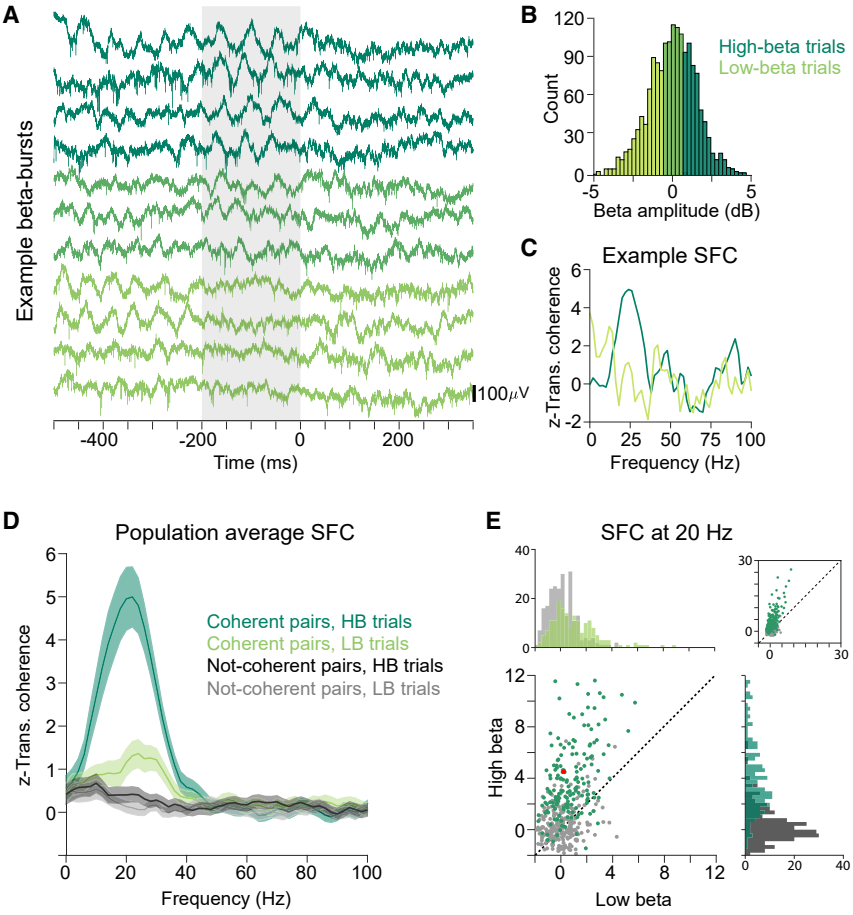

Figure 3. Beta-frequency bursts and coherent neuronal dynamics

(A) Raw extracellular recordings a sample recording site during several LRS task trials. Shaded area denotes the window of interest used for calculating beta amplitude values.

(B) Pretarget beta burst amplitude at the sample site (same as A) on an example experimental session. Dark-green: high-beta trials (HB, ~33% highest beta bursts); light-green: low-beta trials (LB, ~33% lowest beta bursts).

(C) Spike-field coherence (SFC) between an example unit and field recorded on a neighboring electrode (same as A and B).

(D) Population average SFC of coherent pairs (n = 176) and not-coherent pairs (n = 233). The SEM of SFC is shown in lighter shades.

(E) Scatterplot of HB SFC versus LB SFC at 20 Hz. Plot limits are magnified to improve visibility. Inset: all the SFC electrode pairs; each dot denotes a recording pair. Red dot denotes the example SFC in (C). Marginal histograms denote the SFC distribution for HB and LB trials.

Beta bursts selectively modulate exogenous attentional selection during conflict

We asked whether beta bursts modulate attentional selection in general or modulate either exogenous or endogenous attentional selection. We used conflict trials to test the relationship between beta bursts and the neuronal mechanisms of attentional selection and to ask whether beta bursts exhibit specificity for endogenous or exogenous selection. We focused on LRS conflict trials for which the choices were made into the response field of each neuron under study.

We examined three hypotheses. First, since the firing rate of VM neurons reflects both endogenous and exogenous attentional selection, and if LPFC beta bursts modulate attentional selection, the rate of VM neuron firing should differ when beta burst amplitude was high compared with when beta burst amplitude was low. Second, since visual and movement neuron activity does not reflect attentional selection, if beta bursts mediate control of attentional selection, the firing rate of these neurons should not differ on HB and LB trials. Finally, if beta bursts do not modulate selective attention in general and modulate either endogenous or exogenous selection, the relationship between beta bursts and VM neuron firing rate should be present for either endogenous or exogenous selection trials and not both sets of trials.

We observed that VM neuron firing on InRF conflict trials involving exogenous selection significantly differed when pretarget beta burst amplitude was high compared with that when the amplitude was low (Figure 4A, VM-exo: $p < 0.01$, permutation). Visual and movement neuron firing did not differ between HB and LB trials during exogenous selection (InRF-conflict: visual-exo: $p > 0.01$; movement-exo, $p > 0.01$, permutation). This demonstrates that beta bursts in LPFC can modulate attentional selection and do not modulate LPFC firing rates more generally.

Beta bursts selectively modulated exogenous selection and LPFC neuron firing in the response field for HB and LB trials. Beta bursts did not significantly modulate firing activity during endogenous selection, and this was true for all three classes of neuronal response (InRF-conflict: VM-endo, $p > 0.01$; visual-endo, $p > 0.01$; movement-endo, $p > 0.01$, permutation). Beta bursts did not alter VM neurons firing out of the response field (OutRF-conflict trials: VM-exo, $p > 0.01$; VM-endo, $p > 0.01$; visual-exo, $p > 0.01$; visual-endo, $p > 0.01$; movement-exo, $p > 0.01$; movement-endo, $p > 0.01$, permutation, Figures S4A–S4D).

We compared VM neuron firing across all trials with choices into the response field against HB and LB trials (Figures S4F and S4G). On exo-HB trials, VM neuron firing was lower than the average firing rate, and on exo-LB trials VM neuron firing was higher than the average firing rate. This was not observed for endogenous selection trials. Therefore, an increase in pretarget beta activity could suppress luminance processing and a reduction in pre-target beta could facilitate luminance processing selectively on exogenous selection trials.

Beta activity modulated exogenous selection irrespective of the location of RF in the visual field (Figures S4H–S4J). Beta

Please cite this article in press as: Dubey et al., Top-down control of exogenous attentional selection is mediated by beta coherence in prefrontal cortex, Neuron (2023), https://doi.org/10.1016/j.neuron.2023.06.025

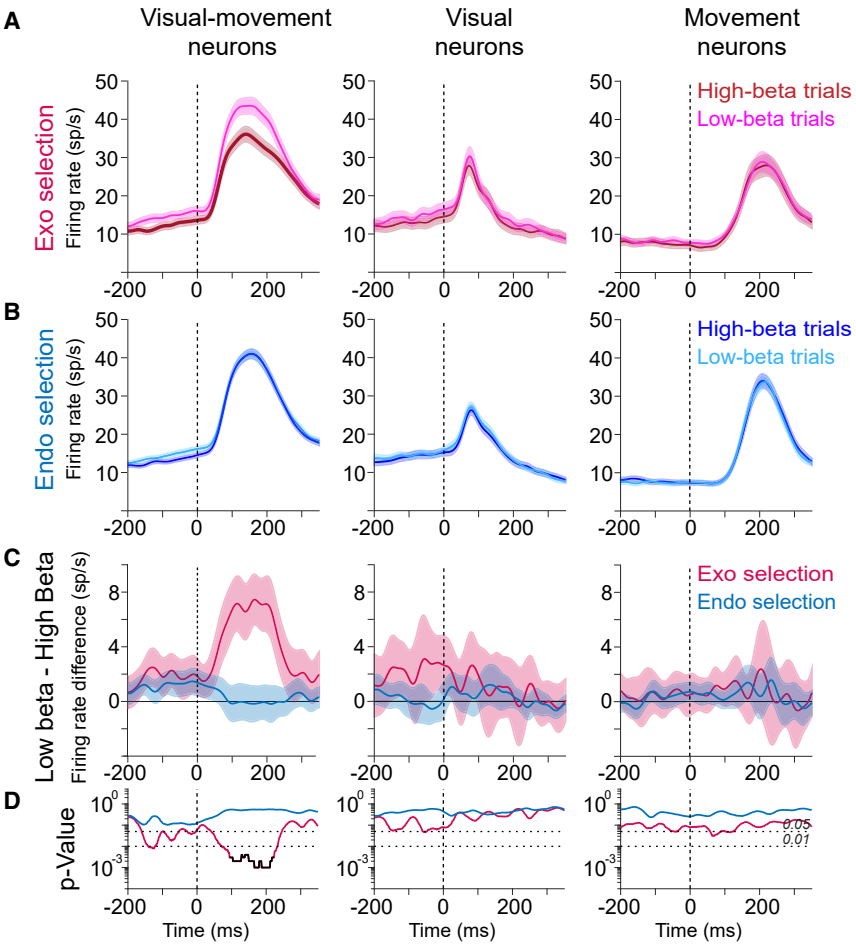

Figure 4. Beta bursts selectively modulate VM neuron firing for exogenous selection during conflict

(A) PSTH of the VM, visual, and movement neurons for exogenous selection when pre-target beta burst is high (HB trials) and low (LB trials). Mean ± SEM are shown for InRF conflict trials when selection was in the RF of the units. Dotted lines denote target onset.

(B) Same as (A) but for endogenous selection.

(C) Difference in firing rates for pre-target low and high beta bursts. Mean ± SEM are shown for exogenous and endogenous selection.

(D) Permutation test p values under a null hypothesis that there is no difference in firing rates for high-beta and low-beta trials for exogenous selection and endogenous selection. FDR corrected p values for alpha = 0.01 (black).

burst modulation effect was not selective to 33% grouping used for selecting HB and LB trials and was observed significantly for other percentiles as well (Figure S5). The modulation of VM neurons firing for exogenous selection was specific to beta frequency range and was not present for alpha (8–13 Hz) and gamma (40–70 Hz) activity (Figure S6). These results demonstrate that pre-target beta activity selectively modulates VM neuron firing for exogenous selection into the response field.

We next asked whether beta burst modulation alters the timing of exogenous selection. Consistent with the suppression of VM neuron firing rate, higher-amplitude beta bursts suppressed the exogenous process in time and delayed the selection by 10 ms on HB trials compared with LB trials (exoHB ST = 54 ms; exoLB ST = 44 ms, p = 0.03 permutation, Figures S7A–S7C). This was not observed for endogenous selection trials (endoHB ST = 121 ms; endoLB ST = 117 ms; p = 0.26, permutation, Figures S7D–S7F). The difference in beta burst amplitude values for HB exogenous and endogenous trials further supported the differences for exogenous and endogenous selection (p = 0.02, rank-sum, Figure S7H). These results demonstrate that beta burst activity modulates both the strength and timing of exogenous attentional selection.

Beta bursts do not modulate exogenous selection in the absence of conflict with endogenous selection

To further investigate beta-burst-related modulation of exogenous selection, we analyzed luminance-only trials (Figure 1Cii). In these trials, there was no conflict present and selection for fast RTs was predominantly guided by the exogenous selection. If beta bursts inhibit exogenous selection in general, then VM neuron firing rate on InRF trials should differ on trials when beta burst amplitude is high compared with when beta burst amplitude is low. Alternatively, if beta bursts specifically inhibit exogenous selection when there is conflict with endogenous selection, the rate of VM neuron firing should not differ on HB and LB trials.

Unlike during LRS conflict trials, the rate of VM neuron firing did not significantly differ for HB and LB trials when the Bright target was selected in the presence of the Dim target and the reward contingencies were the same (Figure 5A, InRF: VM-exo, p > 0.01, permutation; S7J). Visual and movement neuron firing did not differ between HB and LB trials on these trials (Figure 5A, InRF: visual-exo, p > 0.01; movement-exo, p > 0.01, permutation). This demonstrates that pre-target beta bursts in LPFC specifically inhibit exogenous selection when in conflict with endogenous selection and do not modulate exogenous selection in general.

We also analyzed reward-only trials, and the results confirmed that pre-target beta bursts did not modulate LPFC neuron firing rate in the absence of conflict between exogenous and endogenous selection (Figure 5B, InRF trials: VM-endo, p > 0.01; visual-endo, p > 0.01; movement-endo, p > 0.01, permutation).

Pre-target beta burst exogenous attentional modulation is transient in time

Pre-target beta bursts (−200 to 0 ms, where 0 is target onset) selectively inhibit the neuronal mechanisms of exogenous

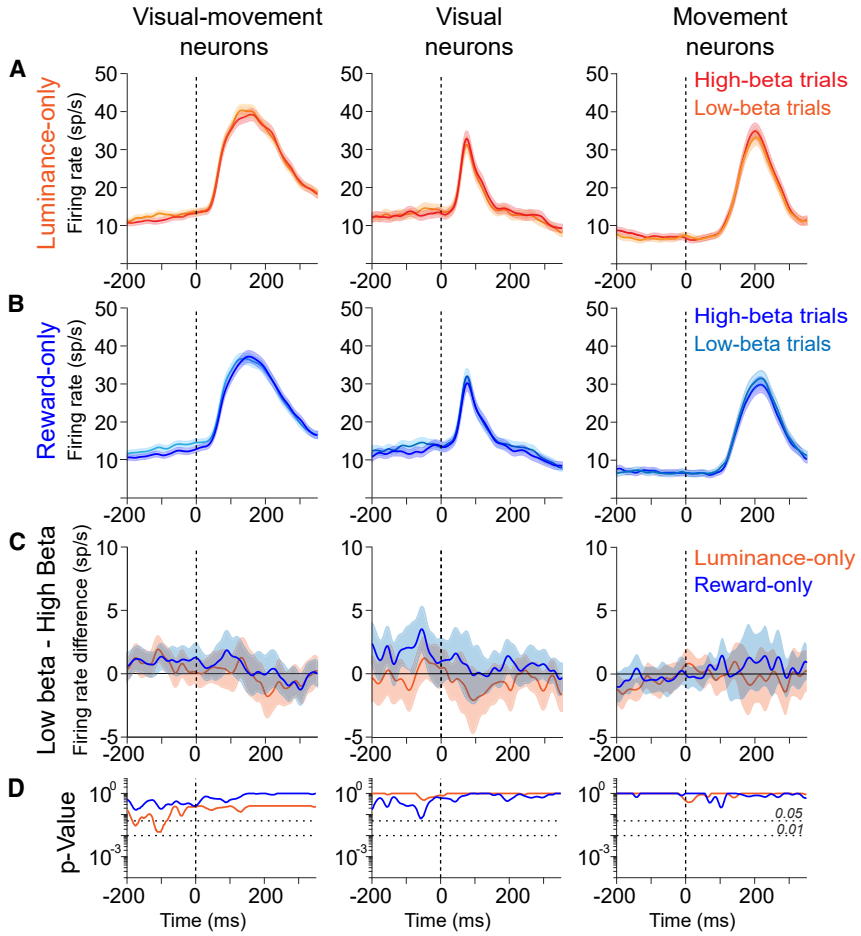

Figure 5. Beta bursts do not modulate exogenous selection when not in conflict with endogenous selection

(A) PSTH of three groups of neurons on luminance-only trials. Mean ± SEM are shown for InRF trials when the Bright target is selected in the RF. Dotted lines denote target onset.

(B) Same as (A), but for reward-only trials. Mean ± SEM are shown for InRF trails when the Rich target is selected in the RF.

(C) Difference in firing rates for high-beta (HB) and low-beta (LB) trials. Mean ± SEM are shown for exogenous and endogenous selection.

(D) Permutation test p values under a null hypothesis that there is no difference in firing rates for HB and LB trials for exogenous selection and endogenous selection.

attentional selection and not of endogenous attentional selection. Since exogenous selection occurs earlier in time (49 ms) compared with endogenous selection (116 ms), the results may simply be due to the proximity in time of beta bursts to exogenous-selection mechanisms. If so, beta bursts that occur later in time, and hence closer to the time of endogenous selection, may instead modulate endogenous selection, not exogenous selection. We analyzed beta bursts during six time epochs and studied VM neuron firing patterns for InRF trials involving endogenous selection when beta burst amplitude was high compared to when the amplitude was low (Figure 6B). VM neuron firing rates on InRF trials were not significantly different between HB and LB trials during the (–100 to 100 ms) epochs (Figures 6C and 6D, endo [–100 to100], $p > 0.01$, permutation).

Examining the time course of beta-burst-related modulation also revealed that early beta bursts do not tend to modulate exogenous attentional selection (Figure 6A). The strongest modulation of VM neuron firing was observed for beta bursts that occurred immediately before target onset (Figure 6C).

Pre-target beta bursts modulate exogenous selection reaction times

If the selective modulation of VM neuron firing with coherent beta activity reflects attentional selection, then the modulatory effect of beta activity on conflict trials should be present during exogenous choice behavior more than during endogenous choice behavior. Since behavioral RTs reflect the underlying mechanism of attentional selection, we specifically predicted that RTs should vary trial by trial with coherent beta activity on exo-conflict trials more than on endo-conflict trials. RTs were correlated with coherent beta activity on exo-conflict trials (M1: rho = 0.32, p = 0.02; M2: rho = 0.79, p = 0, Spearman correlation) as well as on endo-conflict trials (M1: rho = -0.38, $p = 4.1 \times 10^{-3}$; M2, rho = 0.78, p = 0, Spearman correlation). For each monkey, changes in coherent beta activity were associated with changes in RTs on exogenous choice trials more than on endogenous choice trials (Figure 7A). For the exo-conflict group of trials, the RTs significantly differed with coherent beta activity (M1: normalized RT range, 4.65%; absolute RT range, 8.59 ms, p = 0.02; M2: normalized RT range, 2.97%; absolute RT range, 5.54 ms, p = 0.01, permutation). Normalized RT range refers to the percentage range (maxRT–minRT) of variation of RT with beta values. Absolute RT range refers to the range (maxRT–minRT) of variation in millisecond durations. For the endo-conflict group of trials, RTs did not significantly differ with coherent beta activity (M1: normalized-RT range, 1.25%; absolute-RT range, 2.76 ms, p = 0.35; M2: normalized-RT range, 0.95%; absolute-RT range,1.34 ms, p = 0.12, permutation). Finally, since VM neuron firing effects are not present on nonconflict trials, the relationship between beta-activity and RTs should not be present on nonconflict trials. Pre-target coherent beta activity and RTs did not significantly differ when sorting on luminance-only nonconflict trials, but differed significantly when sorting on reward-only nonconflict trials, albeit across a small range of RT compared with exogenous conflict trials (Figure 7B). Results for luminance-only—M1: normalized-RT range, 1.21%; absolute RT range: 2.14 ms, p = 0.47; M2: normalized-RT range, 3.67%; absolute-RT range, 3.78 ms, p = 0.11. Results for reward-only—M1: normalized-RT

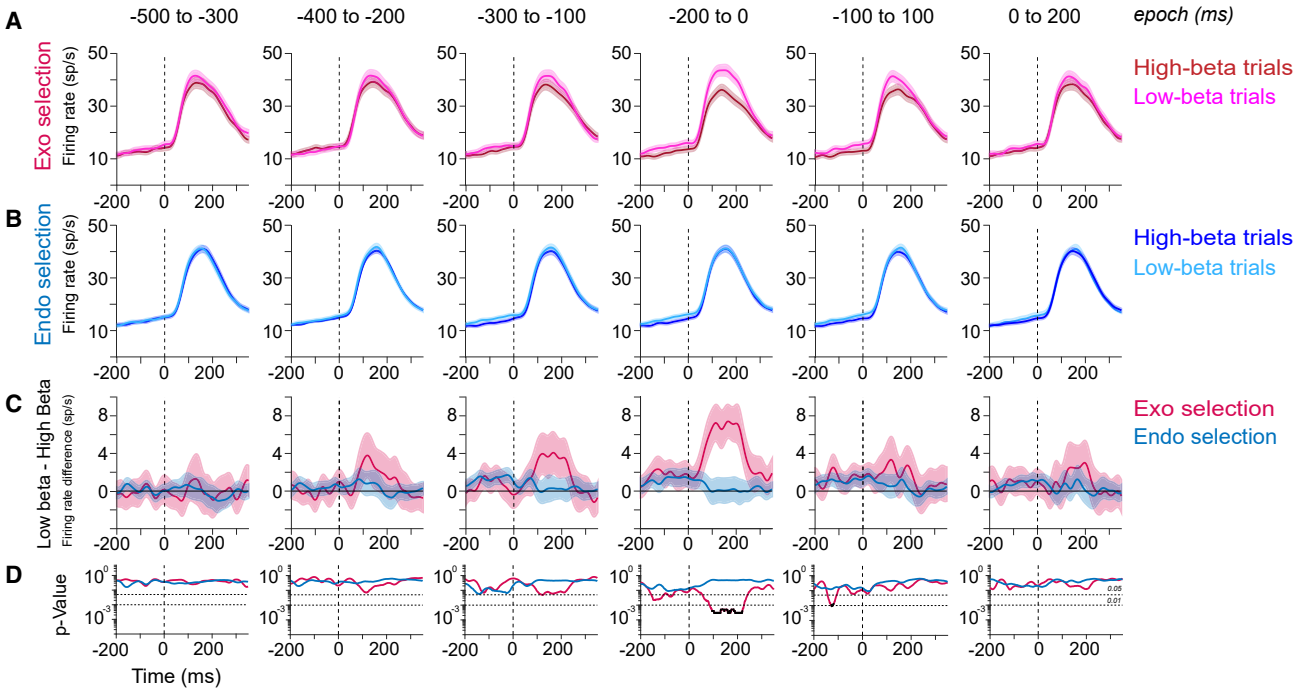

Figure 6. Beta burst exogenous attentional modulation is transient

(A) VM neuron firing activity modulated by HB and LB bursts computed during six different time-windows. Mean ± SEM are shown for exogenous selection when the Poor-Bright target is selected in the RF. Dotted lines denote target onset.

(B) Same as (A), but for endogenous selection. Mean ± SEM are shown for InRF trials when the Rich-Dim target is selected in the RF.

(C) Difference in firing rates for HB and LB trials. Mean ± SEM are shown for exogenous and endogenous selection.

(D) Permutation test p values under a null hypothesis that there is no difference in firing rates for HB and LB trials for exogenous selection and endogenous selection. FDR corrected for p values for 0.01 alpha (black).

range, 2.63%; absolute-RT range, 5.09 ms, p = 0.05; M2: normalized-RT range, 2.32%; absolute-RT range, 4.54 ms, p = 0.02, permutation).

Therefore, the role of coherent beta activity in attentional selection is specifically present during conflict, is generally consistent with the pattern of results observed for the VM neurons, and consequently may mediate top-down control of attentional selection by modulating sensory, cue-driven responses in the VM neuron subpopulation.

DISCUSSION

We make two specific contributions that demonstrate a role for beta-frequency neural coherence in attentional selection through inhibitory mechanisms (Figure 8). We propose that attentional selection involves filtering of luminance and reward channels that communicate information to VM neurons in LPFC in order to select a response (Figure 8A). When beta bursts are not present, target onset drives LPFC to select information in the luminance channel before information in the reward channel is available (Figure 8B). When beta bursts are present, information in the luminance-channel is inhibited and the response tends to be selected based on information in the reward channel (Figure 8C).

We then demonstrate that coherent neuronal activity in the beta-frequency range (15–30 Hz) selectively modulates exogenous selection by suppressing the luminance channel that carries salient sensory information. Beta activity observed in the pre-target period is associated with the inhibited post-target, sensory-driven firing by LPFC neurons when selection is driven by exogenous attention, but not by endogenous attention. Consequently, our results are consistent with the top-down control view of attentional selection. According to the top-down control view, selection of task-relevant endogenous targets relies on mechanisms of multiregional communication that limit the influence of sensory inputs.[11–13] Since top-down control mechanisms operate under the knowledge of task relevance,[13] the beta-activity effect was observed on conflict trials, but not on nonconflict trials. On conflict trials, selection of the task-relevant target yielded high reward, whereas on nonconflict trials the task did not prioritize one target over another based on reward value. Since we show the role played by coherent beta activity could be to modulate information flow due to sensory inputs, our work provides new evidence for how coherent beta activity in LPFC could mediate the top-down control of attentional selection.

We show how coherent beta activity could bias the mechanisms of attentional selection in LPFC by influencing the flow of sensory information during target selection. We specifically show that a subgroup of LPFC neurons, VM neurons, and not visual and movement neurons, encodes both exogenous and endogenous selection. The time scales underlying exogenous and endogenous selection have been a major focus of

Please cite this article in press as: Dubey et al., Top-down control of exogenous attentional selection is mediated by beta coherence in prefrontal cortex, Neuron (2023), https://doi.org/10.1016/j.neuron.2023.06.025

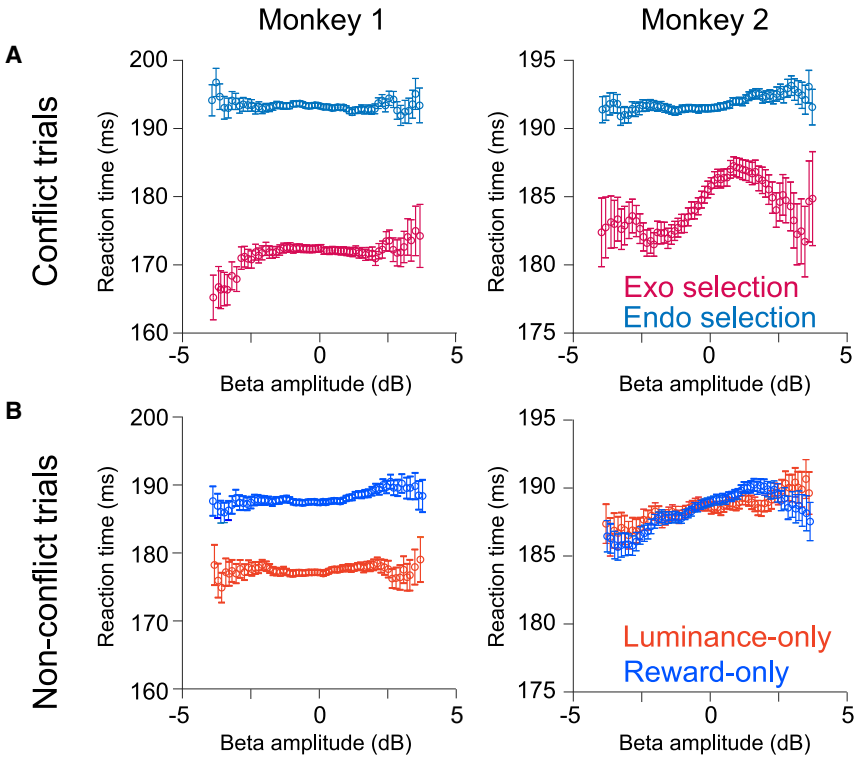

Figure 7. Beta bursts selectively modulate exogenous selection reaction times

(A) Saccade RTs on conflict trials as a function of pretarget beta burst amplitude for monkey 1 and monkey 2. Exogenous selection choices (red); endogenous selection choices (blue).

(B) Same as (A), but for luminance-only and reward-only trials.

behavioral work that has shown that reaction times are typically ~30 ms faster for exogenous selection.[1,2,4,7,39] Here, we go further and also measure the time scales of exogenous and endogenous selection by analyzing the spiking patterns of populations of individual LPFC neurons. Consistent with previous recordings in LPFC,[9] we find that VM neuron spiking activity in response to target onset encoded exogenous selection ~50 ms before endogenous selection. This difference in timing means that coherent beta activity in PFC can have a substantial influence on the direction of sensory information flow and bias the selection of relevant targets in the presence of irrelevant distractors.

In the following, we discuss the mechanisms of top-down attentional control and how coherent beta activity may support the selection of task-relevant targets.

Top-down attentional control mechanisms are mediated by coherent beta activity

In LPFC, beta activity reflects exogenous and endogenous attentional processes.[9,30,32,40] The emergence of LPFC beta activity before selection during different goal-defining tasks further suggests a role for beta activity in the top-down control of attention selection.[11,32,41] Here, we more closely examine the strong relationship between spiking and coherent beta activity in LPFC immediately before presenting relevant and irrelevant targets to reveal mechanisms of top-down attentional control. The central aspect of top-down control is inhibition with knowledge of what needs to be controlled, i.e. relevance.[13] We show that LPFC beta activity is associated with the inhibition of LPFC neural firing during exogenous selection and not endogenous selection, and so is grounded in task-relevance. Importantly, LPFC beta activity mediated selective inhibition was only observed in presence of conflict, i.e., when sensory and reward drive each favored the selection of different targets (Figure 4). In absence of conflict, when sensory information was absent, LPFC firing rates were not modulated with beta activity (Figure 5).

On conflict trials, reward-drive favored the selection of the task-relevant target whereas, on non-conflict trials, absence of reward-drive diminished the task relevance of one target over other. Therefore, we propose that LPFC performs top-down control of attentional selection by deploying beta-frequency coherent neural activity to selectively limit or bias the flow of sensory information specifically when conflicting information drives target selection.

The posterior parietal cortices also process exogenous sensory information.[9,17,41,42] LPFC coherent beta network that selectively inhibits sensory information likely operates across frontal-parietal projections. Indeed, frontal and parietal areas both reflect coherent beta activity indexing stimulus selection in attention and working memory.[9,30,43] LPFC may selectively inhibit PPC information flow through a long-range beta network. If so, prefrontal areas need to generate a sufficiently reliable and impactful neural stimulus to influence posterior parietal areas. The firing of bursts as compared to single isolated spikes offer a candidate mechanism.[44,45] For example, long-range beta burst synchronization between anterior cingulate cortex and LPFC exists during selective attention.[46] Our observations of pre-target beta bursts highlight a potential mechanistic role for how information is routed through PPC during the top-down control of attentional selection.

LRS task reveals the timescale of exogenous and endogenous selection mechanisms

The LRS task revealed the time course of attentional selection mechanisms in LPFC. Use of a non-cue binary-choice task, in which selection immediately followed target onset and both target locations were spatially randomized trial by trial, revealed distinct timescales for each form of attentional selection. Previously used behavioral tasks have often manipulated spatial attention in a delayed design by presenting an attentional cue before the onset of a target.[9,30,47–50] In such paradigms, spatial attention is allocated to the cue location before exogenous or

Please cite this article in press as: Dubey et al., Top-down control of exogenous attentional selection is mediated by beta coherence in prefrontal cortex, Neuron (2023), https://doi.org/10.1016/j.neuron.2023.06.025

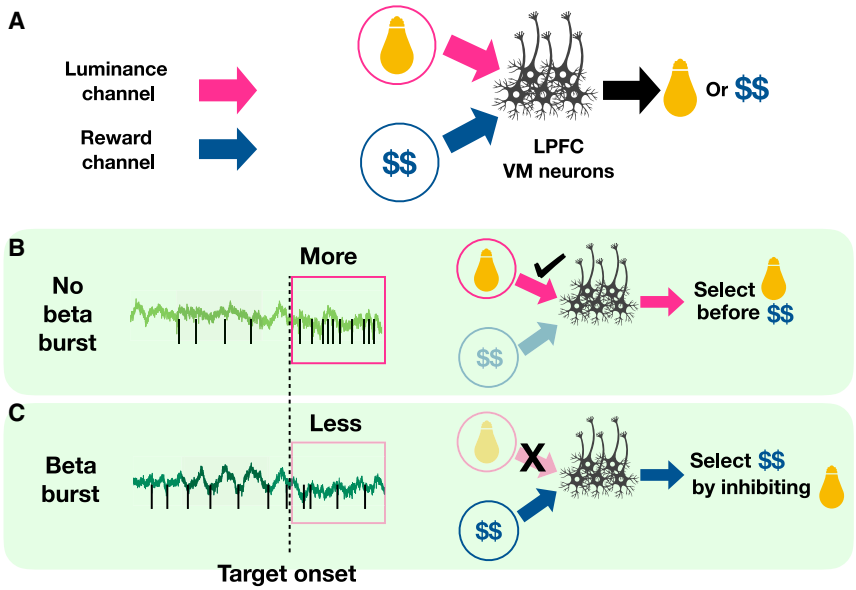

Figure 8. Channel modulation hypothesis

(A) LPFC VM neurons receive luminance and reward information from two distinct communication channels, which compete to guide behavior. Exogenous selection of "Bright" and endogenous selection of "Rich" target depends on inhibitory modulation of the luminance channel.

(B) In the absence of beta bursts, the luminance channel is open, communicating sensory-driven salient information earlier than goal-driven information. Information in the luminance channel drives the exogenous selection of the Bright target.

(C) In the presence of beta bursts, the luminance channel is close, inhibiting communication of sensory information. Information in the reward channel drives the endogenous selection of the Rich target.

endogenous attention is recruited by the target. Previous work has also used tasks in which targets are presented at spatial locations in a predictable manner, which can generate spatial biases in behavior that may also be confounded with attentional selection mechanisms.[48]

While the LRS task was used to dissociate exogenous and endogenous attentional selection mechanisms, previous work has shown that a non-salient target previously associated with reward may also capture attention,[51,52] resulting in an interaction between salience-driven and involuntary value-driven automatic attention. Whether coherent beta activity is implicated in the neural mechanisms of interactions between other forms of attention capture is an interesting direction for further work.

One concern is that the difference in VM neuron firing between the exo- and endo- conditions is simply due to physical brightness of the target and not attentional selection (Figure 2). However, the luminance-only trials control for physical brightness effects. In these trials, physical brightness is the same as in the conflict trials, but the recruitment of exogenous and endogenous attention differs (Figures S2B and S2D). Further, the physical brightness value of the selected target was not correlated to the pre-target beta value (Figures S8A–S8H). Therefore, the beta-modulation effects that we report are most consistent with an attentional effect.

Dynamic interplay of exogenous and endogenous attentional selection

By dynamically shifting between more and less active coherent states, HB and LB, our results show that VM neurons in the coherent beta subnetwork may flexibly modulate multiregional communication across a sensory information channel that carries visual target information into the association cortices. We report behavioral effects in which the influence of coherent beta activity on saccade RTs is consistent with the effects observed in VM neuron firing (Figure 7). Changes in coherent beta activity were associated with changes in RTs on exogenous choice conflict trials more than on endogenous choice conflict trials. On trials when the choice was to the endogenous target, RTs were more similar across trials with beta bursts before target onset that differed in strength. This pattern of results mirrors that for the variations of VM neuron firing with pre-target beta activity across conflict and nonconflict trials. Thus, neural and behavioral results reinforce the flexible interplay between exogenous and endogenous selection associated with beta-mediated modulation of a sensory-driven information channel.

Comparison with previous studies

We categorized the responses of the population of LPFC neurons in terms of three response groups: visual, movement, and VM neurons. To assess the presence of multiple response types, we examined LPFC neuronal response during the LRS task and demonstrated the presence of nonrandom task-relevant structured selectivity (Figures S1F and S1G). Whether the selectivity of frontal cortical neurons is random or nonrandom, as well as whether nonrandom selectivity forms distinct clusters in a high-dimensional space of responses—as opposed to simply a continuum in two-dimensions as we observe—is an interesting topic. Previous studies report that neuronal populations express both random mixed selectivity[53,54] and nonrandom mixed selectivity that form clusters in a high-dimensional space of neuronal responses.[55,56] Consequently, our data are less consistent with random selectivity and are more broadly consistent with Hirokawa et al.,[55] who also show that responses co-vary with task-relevant features. Overall, these analyses support our approach to characterize the population response in terms of multiple response groups.

Previous studies have associated beta activity with inhibition and reach movement initiation.[57–60] In the sensorimotor cortex, beta amplitude increases at rest and in stable postures and reduces during movement.[36,61,62] For example, Kilavik et al. showed increased beta in both pre-cue and pre-go epochs of reach movement tasks, with a temporary drop in beta amplitude after cue.[63] The postcue suppression of beta amplitude for movement planning and initiation may be related to PFC beta before oculomotor selection that we report. However, the detailed pattern of our

results does not suggest that PFC beta is related to the saccade itself. We only observe the beta modulation effects in trials involving conflict. If the results were due to movement suppression, we would also observe them on reward-only and luminance-only trials (Figure 5). In addition, we do not observe beta effects on those PFC neurons whose activity is most tied to the movement—the movement neurons (Figure 4). Furthermore, beta activity altered VM neuron firing for ipsilateral and contralateral saccade selection and was not a lateralized motor effect (Figures S4H–S4J). Finally, we do not observe the effects on trials captured by endogenous attention and only observe the effects on trials with luminance-driven exogenous responses (Figure 4).

Prefrontal beta activity observed during attention and working memory reflects information about the task-relevant rules that determine stimulus-response mapping[9,32,43] using tasks that employ a task rule to match a sample either in object or space feature following a cue/delay period. In comparison, the LRS task employs a non-cue binary-choice task design to examine attentional selection mechanisms. The beta burst modulation effect we report could be due to differences in involvement of beta activity in the preparatory period and cue-triggered delay period. However, we propose that conflict between the two sources of information influences the attentional selection process irrespective of the beta activity period cue-triggered/preparatory beta. The channel modulation top-down control model (Figure 8) suggests that beta activity is involved in resolving conflict. Therefore, cue-period beta-activity may also influence the selection process in the presence of conflict.

Previous studies have suggested that LPFC neuron firing activity is modulated by reward value.[64,65] We did not observe a value-based modulation of VM neuron firing activity (Figures S2I and S2J). However, we did observe value-based modulations in movement neuron firing. Movement neuron firing was greater when the rich target was selected InRF compared with poor target selection InRF. Movement neuron firing during our task likely does not reflect endogenous attention processing and may instead reflect a form of reward expectancy. Note, however, the increased firing for the rich target contradicts work by Kaping et al., which reports enhanced LPFC activity when a low-value target is selected over a high-value target. This discrepancy could arise from our use of an immediate saccade, unlike other work involving covert attentional cues.

In conclusion, we reveal that the mechanisms of top-down control of attentional selection in LPFC involve the inhibition of luminance information to facilitate reward-guided behavior. We show that the dynamics of a population of VM neurons that fire coherently with beta activity may mediate top-down control of attentional selection, consistent with a role in inhibitory multiregional communication. We further show that coherent beta activity selectively modulates exogenous responding compared with endogenous responding, resulting in the flexible interplay between exogenous and endogenous selection necessary to resolve conflict.

STAR★METHODS

Detailed methods are provided in the online version of this paper and include the following:

SUPPLEMENTAL INFORMATION

Supplemental information can be found online at https://doi.org/10.1016/j.neuron.2023.06.025.

ACKNOWLEDGEMENTS

We would like to thank Gerardo Moreno for surgical assistance, Roch Comeau, Stephen Frey, and Brian Hynes for custom modifications to the BrainSight system, and members of the Pesaran lab for helpful feedback. We thank Supratim Ray for insightful comments on an earlier version of this manuscript. This work was supported in part by NIH Ruth L. Kirschstein National Service award F32-MH100884 from the National Institute of Mental Health (NIMH) (D.A.M.), a Swartz Fellowship in Theoretical Neurobiology (D.A.M.), NIH Training Grant T32-EY007158 (D.A.M.), R01-NS104923 (B.P.), UF1-NS122123 (B.P.), and MURI W911NF-16-1-0368 (B.P.).

AUTHOR CONTRIBUTIONS

Conceptualization, A.D., D.A.M., and B.P.; methodology, A.D., D.A.M., and B.P.; investigation, A.D., D.A.M., and B.P.; formal analysis, A.D. and B.P.; writing – original draft, A.D. and B.P.; writing – review and editing, A.D., D.A.M., and B.P.; funding acquisition, D.A.M. and B.P.; supervision, B.P.

DECLARATION OF INTERESTS

The authors declare no competing interests.

Received: June 1, 2022
Revised: November 30, 2022
Accepted: June 26, 2023
Published: July 26, 2023

REFERENCES

1. Corbetta, M., and Shulman, G.L. (2002). Control of goal-directed and stimulus-driven attention in the brain. Nat. Rev. Neurosci. *3*, 201–215.
2. Theeuwes, J. (2010). Top-down and bottom-up control of visual selection. Acta Psychol. *135*, 77–99.
3. Carrasco, M., Ling, S., and Read, S. (2004). Attention alters appearance. Nat. Neurosci. *7*, 308–313.
4. Awh, E., Armstrong, K.M., and Moore, T. (2006). Visual and oculomotor selection: links, causes and implications for spatial attention. Trends Cogn. Sci. *10*, 124–130.

5. Corbetta, M., Akbudak, E., Conturo, T.E., Snyder, A.Z., Ollinger, J.M., Drury, H.A., Linenweber, M.R., Petersen, S.E., Raichle, M.E., Van Essen, D.C., et al. (1998). A common network of functional areas for attention and eye movements. Neuron *21*, 761–773.
6. Moore, T., and Zirnsak, M. (2017). Neural mechanisms of selective visual attention. Annu. Rev. Psychol. *68*, 47–72.
7. Markowitz, D.A., Shewcraft, R.A., Wong, Y.T., and Pesaran, B. (2011). Competition for visual selection in the oculomotor system. J. Neurosci. *31*, 9298–9306.
8. Dugué, L., Merriam, E.P., Heeger, D.J., and Carrasco, M. (2020). Differential impact of endogenous and exogenous attention on activity in human visual cortex. Sci. Rep. *10*, 21274.
9. Buschman, T.J., and Miller, E.K. (2007). Top-down versus bottom-up control of attention in the prefrontal and posterior parietal cortices. Science *315*, 1860–1862.
10. Pesaran, B., Hagan, M., Qiao, S., and Shewcraft, R. (2021). Multiregional communication and the channel modulation hypothesis. Curr. Opin. Neurobiol. *66*, 250–257.
11. Womelsdorf, T., and Everling, S. (2015). Long-range attention networks: circuit motifs underlying endogenously controlled stimulus selection. Trends Neurosci. *38*, 682–700.
12. Anderson, M.C., and Weaver, C. (2009). Inhibitory control over action and memory. In Encyclopedia of Neuroscience (Academic Press), pp. 153–163. https://doi.org/10.1016/b978-008045046-9.00421-6.
13. Miller, E.K., and Cohen, J.D. (2001). An integrative theory of prefrontal cortex function. Annu. Rev. Neurosci. *24*, 167–202.
14. Buschman, T.J., and Kastner, S. (2015). From behavior to neural dynamics: an integrated theory of attention. Neuron *88*, 127–144.
15. Moore, T., and Armstrong, K.M. (2003). Selective gating of visual signals by microstimulation of frontal cortex. Nature *421*, 370–373.
16. Miller, E.K. (2000). The prefrontal cortex and cognitive control. Nat. Rev. Neurosci. *1*, 59–65.
17. Suzuki, M., and Gottlieb, J. (2013). Distinct neural mechanisms of distractor suppression in the frontal and parietal lobe. Nat. Neurosci. *16*, 98–104.
18. Paneri, S., and Gregoriou, G.G. (2017). Top-down control of visual attention by the prefrontal cortex. Functional specialization and long-range interactions. Front. Neurosci. *11*, 545.
19. Gregoriou, G.G., Rossi, A.F., Ungerleider, L.G., and Desimone, R. (2014). Lesions of prefrontal cortex reduce attentional modulation of neuronal responses and synchrony in V4. Nat. Neurosci. *17*, 1003–1011.
20. Petrides, M. (2005). Lateral prefrontal cortex: architectonic and functional organization. Philos. Trans. R. Soc. Lond. B Biol. Sci. *360*, 781–795.
21. Rushworth, M.F.S., Buckley, M.J., Gough, P.M., Alexander, I.H., Kyriazis, D., McDonald, K.R., and Passingham, R.E. (2005). Attentional selection and action selection in the ventral and orbital prefrontal cortex. J. Neurosci. *25*, 11628–11636.
22. Rossi, A.F., Bichot, N.P., Desimone, R., and Ungerleider, L.G. (2007). Top down attentional deficits in macaques with lesions of lateral prefrontal cortex. J. Neurosci. *27*, 11306–11314.
23. Buckley, M.J., Mansouri, F.A., Hoda, H., Mahboubi, M., Browning, P.G.F., Kwok, S.C., Phillips, A., and Tanaka, K. (2009). Dissociable components of rule-guided behavior depend on distinct medial and prefrontal regions. Science *325*, 52–58.
24. Petrides, M., and Pandya, D.N. (1994). Comparative architectonic analysis of the human and the macaque frontal cortex. In Handbook of Neuropsychology (Elsevier), pp. 17–58.
25. Pesaran, B., Vinck, M., Einevoll, G.T., Sirota, A., Fries, P., Siegel, M., Truccolo, W., Schroeder, C.E., and Srinivasan, R. (2018). Investigating large-scale brain dynamics using field potential recordings: analysis and interpretation. Nat. Neurosci. *21*, 903–919.
26. Hagan, M.A., and Pesaran, B. (2022). Modulation of inhibitory communication coordinates looking and reaching. Nature *604*, 708–713.
27. Voloh, B., and Womelsdorf, T. (2016). A role of phase-resetting in coordinating large scale neural networks during attention and goal-directed behavior. Front. Syst. Neurosci. *10*, 18.
28. Staudigl, T., Minxha, J., Mamelak, A.N., Gothard, K.M., and Rutishauser, U. (2022). Saccade-related neural communication in the human medial temporal lobe is modulated by the social relevance of stimuli. Sci. Adv. *8*, eabl6037.
29. Panichello, M.F., and Buschman, T.J. (2021). Shared mechanisms underlie the control of working memory and attention. Nature *592*, 601–605.
30. Fiebelkorn, I.C., and Kastner, S. (2021). Spike timing in the attention network predicts behavioral outcome prior to target selection. Neuron *109*, 177–188.e4.
31. Antzoulatos, E.G., and Miller, E.K. (2016). Synchronous beta rhythms of frontoparietal networks support only behaviorally relevant representations. eLife *5*. https://doi.org/10.7554/eLife.17822.
32. Buschman, T.J., Denovellis, E.L., Diogo, C., Bullock, D., and Miller, E.K. (2012). Synchronous oscillatory neural ensembles for rules in the prefrontal cortex. Neuron *76*, 838–846.
33. Miller, E.K., Lundqvist, M., and Bastos, A.M. (2018). Working memory 2.0. Neuron *100*, 463–475.
34. Hanslmayr, S., Matuschek, J., and Fellner, M.C. (2014). Entrainment of prefrontal beta oscillations induces an endogenous echo and impairs memory formation. Curr. Biol. *24*, 904–909.
35. Lundqvist, M., Herman, P., Warden, M.R., Brincat, S.L., and Miller, E.K. (2018). Gamma and beta bursts during working memory readout suggest roles in its volitional control. Nat. Commun. *9*, 394.
36. Schmidt, R., Herrojo Ruiz, M., Kilavik, B.E., Lundqvist, M., Starr, P.A., and Aron, A.R. (2019). Beta oscillations in working memory, executive control of movement and thought, and sensorimotor function. J. Neurosci. *39*, 8231–8238.
37. Spitzer, B., and Haegens, S. (2017). Beyond the status quo: a role for beta oscillations in endogenous content (re)activation. eNeuro *4*. https://doi.org/10.1523/ENEURO.0170-17.2017.
38. Funahashi, S., Bruce, C.J., and Goldman-Rakic, P.S. (1989). Mnemonic coding of visual space in the monkey's dorsolateral prefrontal cortex. J. Neurophysiol. *61*, 331–349.
39. Carrasco, M. (2011). Visual attention: the past 25 years. Vision Res. *51*, 1484–1525.
40. Bastos, A.M., Vezoli, J., Bosman, C.A., Schoffelen, J.M., Oostenveld, R., Dowdall, J.R., De Weerd, P., Kennedy, H., and Fries, P. (2015). Visual areas exert feedforward and feedback influences through distinct frequency channels. Neuron *85*, 390–401.
41. Chen, X., Zirnsak, M., Vega, G.M., Govil, E., Lomber, S.G., and Moore, T. (2020). Parietal cortex regulates visual salience and salience-driven behavior. Neuron *106*, 177–187.e4.
42. Gottlieb, J.P., Kusunoki, M., and Goldberg, M.E. (1998). The representation of visual salience in monkey parietal cortex. Nature *391*, 481–484.
43. Salazar, R.F., Dotson, N.M., Bressler, S.L., and Gray, C.M. (2012). Content-specific fronto-parietal synchronization during visual working memory. Science *338*, 1097–1100.
44. Lisman, J.E. (1997). Bursts as a unit of neural information: making unreliable synapses reliable. Trends Neurosci. *20*, 38–43.
45. Ardid, S., Vinck, M., Kaping, D., Marquez, S., Everling, S., and Womelsdorf, T. (2015). Mapping of functionally characterized cell classes onto canonical circuit operations in primate prefrontal cortex. J. Neurosci. *35*, 2975–2991.
46. Womelsdorf, T., Ardid, S., Everling, S., and Valiante, T.A. (2014). Burst firing synchronizes prefrontal and anterior cingulate cortex during attentional control. Curr. Biol. *24*, 2613–2621.
47. Reynolds, J.H., Chelazzi, L., and Desimone, R. (1999). Competitive mechanisms subserve attention in macaque areas V2 and V4. J. Neurosci. *19*, 1736–1753.

48. Liu, T., Abrams, J., and Carrasco, M. (2009). Voluntary attention enhances contrast appearance. Psychol. Sci. *20*, 354–362.

49. Fiebelkorn, I.C., Pinsk, M.A., and Kastner, S. (2018). A dynamic interplay within the frontoparietal network underlies rhythmic spatial attention. Neuron *99*, 842–853.e8.

50. Bisley, J.W., and Goldberg, M.E. (2003). Neuronal activity in the lateral intraparietal area and spatial attention. Science *299*, 81–86.

51. Anderson, B.A., Laurent, P.A., and Yantis, S. (2011). Value-driven attentional capture. Proc. Natl. Acad. Sci. USA *108*, 10367–10371.

52. Jahfari, S., and Theeuwes, J. (2017). Sensitivity to value-driven attention is predicted by how we learn from value. Psychon. Bull. Rev. *24*, 408–415.

53. Rigotti, M., Barak, O., Warden, M.R., Wang, X.J., Daw, N.D., Miller, E.K., and Fusi, S. (2013). The importance of mixed selectivity in complex cognitive tasks. Nature *497*, 585–590.

54. Raposo, D., Kaufman, M.T., and Churchland, A.K. (2014). A category-free neural population supports evolving demands during decision-making. Nat. Neurosci. *17*, 1784–1792.

55. Hirokawa, J., Vaughan, A., Masset, P., Ott, T., and Kepecs, A. (2019). Frontal cortex neuron types categorically encode single decision variables. Nature *576*, 446–451.

56. Yang, W., Tipparaju, S.L., Chen, G., and Li, N. (2022). Thalamus-driven functional populations in frontal cortex support decision-making. Nat. Neurosci. *25*, 1339–1352.

57. Hagan, M.A., Dean, H.L., and Pesaran, B. (2012). Spike-field activity in parietal area LIP during coordinated reach and saccade movements. J. Neurophysiol. *107*, 1275–1290.

58. Dean, H.L., Hagan, M.A., and Pesaran, B. (2012). Only coherent spiking in posterior parietal cortex coordinates looking and reaching. Neuron *73*, 829–841.

59. Pape, A.A., and Siegel, M. (2016). Motor cortex activity predicts response alternation during sensorimotor decisions. Nat. Commun. *7*, 13098.

60. Sanes, J.N., and Donoghue, J.P. (1993). Oscillations in local field potentials of the primate motor cortex during voluntary movement. Proc. Natl. Acad. Sci. USA *90*, 4470–4474.

61. Kilavik, B.E., Zaepffel, M., Brovelli, A., MacKay, W.A., and Riehle, A. (2013). The ups and downs of β oscillations in sensorimotor cortex. Exp. Neurol. *245*, 15–26.

62. Cassim, F., Monaca, C., Szurhaj, W., Bourriez, J.L., Defebvre, L., Derambure, P., and Guieu, J.D. (2001). Does post-movement beta synchronization reflect an idling motor cortex? NeuroReport *12*, 3859–3863.

63. Kilavik, B.E., Ponce-Alvarez, A., Trachel, R., Confais, J., Takerkart, S., and Riehle, A. (2012). Context-related frequency modulations of macaque motor cortical LFP beta oscillations. Cereb. Cortex *22*, 2148–2159.

64. Leon, M.I., and Shadlen, M.N. (1999). Effect of expected reward magnitude on the response of neurons in the dorsolateral prefrontal cortex of the macaque. Neuron *24*, 415–425.

65. Kaping, D., Vinck, M., Hutchison, R.M., Everling, S., and Womelsdorf, T. (2011). Specific contributions of ventromedial, anterior cingulate, and lateral prefrontal cortex for attentional selection and stimulus valuation. PLoS Biol. *9*, e1001224.

66. Markowitz, D.A., Curtis, C.E., and Pesaran, B. (2015). Multiple component networks support working memory in prefrontal cortex. Proc. Natl. Acad. Sci. USA *112*, 11084–11089.

67. Benjamini, Y., and Hochberg, Y. (1995). Controlling the false discovery rate: a practical and powerful approach to multiple testing. J. R. Stat. Soc., B: Stat. *57*, 289–300.

68. Mitra, P.P., and Pesaran, B. (1999). Analysis of dynamic brain imaging data. Biophys. J. *76*, 691–708.

69. Pesaran, B., Pezaris, J.S., Sahani, M., Mitra, P.P., and Andersen, R.A. (2002). Temporal structure in neuronal activity during working memory in macaque parietal cortex. Nat. Neurosci. *5*, 805–811.

70. Maris, E., Schoffelen, J.M., and Fries, P. (2007). Nonparametric statistical testing of coherence differences. J. Neurosci. Methods *163*, 161–175.

Please cite this article in press as: Dubey et al., Top-down control of exogenous attentional selection is mediated by beta coherence in prefrontal cortex, Neuron (2023), https://doi.org/10.1016/j.neuron.2023.06.025

STAR★METHODS

KEY RESOURCES TABLE

REAGENT or RESOURCE	SOURCE	IDENTIFIER
Deposited data		
Experimental data	Recorded experimental data	https://doi.org/10.6084/m9.figshare.23567439.v1
Experimental models: Organisms/strains		
Rhesus macaque (Macaca mulatta)	Covance and Charles River Laboratories	N/A
Software and algorithms		
Analysis code	Custom software analysis code	https://doi.org/10.6084/m9.figshare.23503767.v2
MATLAB R2017	Mathworks	https://www.mathworks.com/products/matlab.html
FSL	Analysis Group, FMRIB, Oxford, UK	https://fsl.fmrib.ox.ac.uk/fsl/fslwiki/
Other		
Microelectrodes 0.7-1.4 MΩ impedance	Alpha Omega single electrodes	https://www.alphaomega-eng.com/
Neural recordings and amplifier for monkeys 1 and 2	NSpike NDAQ system, Harvard Instrumentation	http://nspike.sourceforge.net/#Overview
Eye tracking	ISCAN, MA	http://iscaninc.com
Task controller	Custom LabView software with a real-time embedded system NI PXI-8820	https://www.ni.com/en-us/shop/labview.html

RESOURCE AVAILABILITY

Lead contact

Further information and requests for resources should be directed to and will be fulfilled by the Lead Contact, Bijan Pesaran (pesaran@upenn.edu).

Materials availability

The study did not generate new unique reagents.

Data and code availability

- The electrophysiological and behavioral data reported in this study have been deposited at Figshare. The DOI is listed in the key resources table.
- All original code to analyze the electrophysiological and behavioral data has been deposited at Figshare and is publicly available as of the date of publication. DOIs are listed in the key resources table.
- Any additional information required to reanalyze the data reported in this paper is available from the lead contact upon request.

EXPERIMENTAL MODEL AND STUDY PARTICIPANT DETAILS

All surgical and animal care procedures were done in accordance with National Institute of Health guidelines and were approved by the New York University Animal Care and Use Committee. Two adult male rhesus monkeys (*Macaca mulatta*) participated in the experiments (Monkey 1, 9.5 kg and Monkey 2, 8.4 kg). Both animals had been previously used in other eye-movement experiments.[7,66]

METHOD DETAILS

Experimental preparation

Once trained on behavioral tasks, each animal was implanted with a low-profile recording chamber (Gray Matter Research, MT). The craniotomy was made over the right pre-arcuate cortex of each animal using image-guided stereotaxic surgical techniques (Brainsight, Rogue Research, Canada). A semichronic microelectrode array microdrive (SC32-1, Gray Matter Research, MT) was inserted

Please cite this article in press as: Dubey et al., Top-down control of exogenous attentional selection is mediated by beta coherence in prefrontal cortex, Neuron (2023), https://doi.org/10.1016/j.neuron.2023.06.025

into the recording chamber and sealed. The SC32-1 system has 32 microelectrodes, spaced 1.5 mm away (Figure 1D). The SC32-1 is a modular, replaceable system capable of independent bidirectional control of 32 microelectrodes.

Behavioral experiments

Experimental hardware and software

Eye position was constantly monitored with an infrared optical eye tracking system sampling at 120 Hz (ISCAN). Visual stimuli were presented on an LCD screen (Dell Inc) placed 34 cm from the animal's eyes. The visual stimuli were controlled via custom LabVIEW (National Instruments) software executed on a real-time embedded system (NI PXI-8184, National Instruments).

Experimental design

Each monkey first performed a visually-guided oculomotor delayed response (ODR) task to map the spatial response fields of neurons. Each monkey then performed the luminance-reward-selection (LRS) task to study the flexible control of attentional selection. Behavior and neural data was recorded across 39 (Monkey 1) and 42 (Monkey 2) experimental sessions.

ODR task

Each trial began with a visual fixation target presented at the center of the screen. Each animal maintained fixation for a variable 500-800 ms baseline period. After the baseline period, a red square appeared in the periphery to indicate target location of the saccade. There were eight possible iso-eccentric target locations spaced 10 deg around central fixation. Target location was randomized over trials so that animals could not predict where the cue would appear on any given trial. Each monkey maintained fixation for a variable 1000-1500 ms delay period. After the delay period, the central fixation square was extinguished, providing the Go signal for the animal to move his eyes to the target location. A fluid reward was awarded on successful completion of the trial. A trial was aborted if the animal failed to align his gaze within 2deg of the center of fixation or periphery target. On a given experimental session, on average M1 95 +/- 24 trials performed trials and M2 performed 248 +/- 32 ODR trials (mean +/- sd).

LRS task

Each trial again started with fixation at a visual target at the center of the screen for a variable 500-800 ms baseline period. After the baseline period, the center fixation target was extinguished, and two red targets (T1 and T2) were presented at random locations in the visual periphery at a 10 deg eccentricity from the central fixation. Two targets were constrained to be at least 90 deg apart on each trial. The randomized spatial location of targets controlled for the influence of spatial attention at the start of each trial. Onset of targets provided the animal Go signal to perform a saccade to one of the targets. Each animal was required to maintain a fixation of 300 ms at the chosen target, after which appropriate juice reward was delivered. Each trial lasted 890-1400 ms, and only one choice could be made per trial. A trial was aborted if the animal failed to align his gaze within 2deg of the center of fixation or choice targets. On a given experimental session, on average M1 performed 1276 +/- 348 and M2 performed 1677 +/- 139 (mean +/- sd) LRS trials.

T1 and T2 were two identical in size rectangular stimuli (3-to-1 aspect ratio) with different orientation (Figure 1B). T1 was oriented so that the long axis was vertical and T2 was oriented so that the long axis is horizontal. Long axis of each target subtended 2 deg of visual arc. Two targets were associated with different liquid reward values. Each animal was motivated to select the target associated with the highest value of liquid reward. Mean value of the liquid reward associated with each target was kept constant for blocks of 40-70 trials (Figure 1C). The block transition was unsignaled. Mean reward values varied between 0.04 ml/trial and 0.21 ml/trial. On each trial, a Gaussian-distributed variability (SD = 0.015 ml) was added to the value with each target. Variable reward values further increased animal's uncertainty about the times of reward block transitions. Since the choice behavior around each reward block transition was more exploratory (Figure S8I), we performed all the analysis after excluding the first 10 trials after the block transition. This ensured that the animals followed the reward contingencies.

On each trial, target luminance values were randomly assigned. T1 luminance was randomly assigned from a log-uniform distribution of values ranging from 0.01 to 12.15 cd/m^2. The minimum luminance value was set above the psychophysical threshold for stimulus detection titrated during the ODR task. After the T1 luminance was assigned, the luminance of T2 was assigned such that mean luminance across both targets was 6 cd/m^2. On each trial, target luminance values were assigned independently from the rewards associated with T1 and T2. Additionally, the randomized spatial locations of two targets ensured that the target location of the high-reward and low-luminance target could not be determined from the low-reward and high-luminance target.

Trial-by-trial independent manipulation of luminance and reward values randomly yielded either congruent or conflict set of trials. On a given experimental session, on average Monkey 1 performed 322 +/- 74 congruent trials and 317 +/- 81 conflict trials; Monkey 2 performed 392 +/- 33 congruent trials and 392 +/- 39 conflict trials (mean +/- sd).

On congruent trials, luminance and reward values were both high for one target (Rich-Bright) and were both low for the other target (Poor-Dim). Each monkey showed a strong preference for selecting Rich-Bright target compared to Poor-Dim target (M1: 84% total trials: 9881; M2: 72% total trials 15615: across 39 and 42 experimental sessions).

On conflict trials, however, one target had high-reward and low-luminance (Rich-Dim) and the other target had low-reward and high-luminance (Poor-Bright). Conflict trials, when endogenous selection was expressed and Rich-Dim target was selected were termed as endo-conflict trials (on average each monkey performed M1=211 +/- 62, M2= 301+/- 44 endo-conflict trials per experimental session, mean +/- sd). Similarly, conflict trials when exogenous selection was expressed and Poor-Bright was selected, were termed exo trials (on average each monkey performed M1=107 +/- 47, M2= 91 +/- 25 exo-conflict trials per experimental session, mean +/- sd). Each monkey followed rewards and showed preference for selecting Rich-Dim target compared to Poor-Bright target (M1: 68% total trials: 9751; M2: 77% total trials: 15652 trials, across 39 and 42 experimental sessions).

Interestingly, M2 behavioral performance was better on congruent trials compared to conflict trials. We attribute the difference in M2 performance on conflict vs congruent trials to the role of a shape bias. On conflict trials, M2 preferred T1 compared to T2 (pT1= 82%, pT2= 73%) but this shape preference was not as strong on congruent trials (pT1 = 76%, pT2=73%). Conflict-specific shape preference explains the effect because the preference results in better performance for T1 on conflict trials compared with congruent trials (pT1-conflict = 82%; pT1-congruent = 76 %) but not for T2 (pT2-conflict = 73%; pT2-congruent = 73 %). On each trial, there are three sources of choice information: shape bias, luminance, and experience-dependent reward. On congruent trials, the luminance and reward information agree and so the shape bias does not tend to alter decisions and is not revealed on average- the effect is subthreshold. On conflict trials, the luminance and reward information disagree and so the shape bias tends to alter the decisions and is revealed on average- the effect rises above the threshold. Consequently, the difference in performance between conflict and congruent trials is due to the presence of shape bias in a manner that is consistent with the conceptual framework of the LRS task.

On each experimental session, on a subset of trials, the LRS task featured non-conflict reward-only and luminance-only trials. On reward-only trials, the luminance values of two targets were kept the same for blocks. On luminance-only trials, the average reward values associated with two targets were kept the same for blocks. On a given experimental session, on average Monkey 1 performed 220 +/- 98 reward-only trials and 294 +/- 120 luminance-only trials and Monkey 2 performed 245 +/- 29 reward-only trials and 337 +/- 57 luminance-only trials (mean +/- sd).

Neurophysiological experiments

Recording protocol and data acquisition

Neural recordings were made with glass-coated tungsten electrodes (Alpha Omega, Israel) with impedance 0.7-1.5 M measured at 1 kHz (Bak Electronics, MD). Neural signals were preamplified (10 x gain; Multichannel Systems, Germany), amplified and digitized (16 bits at 30 kHz; NSpike, Harvard Instrumentation Lab), and continuously streamed to disk during the experiment (custom C and Matlab code). Neural recordings were referenced to a ground screw implanted in the left occipital lobe, with the tip of the screw just piercing through the dura mater.

In each animal, electrodes were advanced in each recording session to maximize the yield of isolated single units. Electrodes were advanced through a silastic membrane in the recording chamber, the dura mater and pia before entering the cortex. Each electrode was advanced sequentially in increments of 15 microns, 10 minutes apart to give the electrode time to settle in the tissue. Initial action potentials were recorded at a median depth of 3 mm (2.23 mm in M1; 3.04 mm in M2). Electrodes were gradually advanced across sessions (on average 34 μm/day in M1 and 100 μm/day in M2) until action potentials were no longer present, indicating passage into white matter. Neural recordings were made up to a median distance of 6 mm from their initial position.

Local field potential (LFP) activity was obtained offline by low-pass filtering the broadband raw recording at 300 Hz using a multitaper filter with a 1.5 ms time window. The low-pass filtered LFP activity was further downsampled to 1 kHz from 30 kHz. Multiunit activity (MUA) was obtained by high-pass filtering the raw recordings at 300 Hz and maintaining the original 30 kHz sampling rate. Single unit activity (SUA) was isolated by thresholding MUA activity at 3.5 standard deviations below the mean, performing a principal component analysis of putative spike waveforms, over-clustering these waveforms in PCA using k-means and then merging clusters based on visual inspection. Spike-sorting was performed for each recording session using custom Matlab code (Mathworks). Non-stationarity in recordings were accounted for by performing spike-sorting in 100 ms moving windows. Trials on which spike-clusters were not isolated were removed from further analysis.

Neuronal databases

We advanced electrodes to isolate and record 746 units (M1: 384; M2: 362 units) during the ODR task. Out of 746 units, we further selected 409 (M1: 179; M2: 230 units) single units that were responsive to the LRS task. We selected units with firing rates greater than 5 sp/s in 0 to 200 ms epoch after onset of targets for the LRS task.

Each neuron's response-field (RF) was mapped using the ODR saccade task to eight possible target locations. LPFC neurons showed increased firing in response to target onset alone, saccadic eye movement alone or both target onset and saccadic eye movement (Figures S1A–S1C). Therefore, we computed each neuron's trial-averaged baseline subtracted firing rate in response to eight target locations around target onset and saccade onset (Target onset: baseline epoch = [-200 0ms], stimulus epoch = [0 100ms] and [75 200ms] where 0ms is targets onset; Saccade onset: baseline epoch = [-400 200ms], stimulus epoch = [-50 70ms] where 0ms is saccade onset). We used these epochs to accommodate the firing activity of visual, visual-movement (VM) and movement neurons (Figures 1 and S1A–S1C). Each neuron's RF was estimated against the null hypothesis that there is no difference in response firing rate with respect to baseline, using a permutation test. The baseline-subtracted firing rate at each target's location was compared with the null distribution. Null distribution was generated by shuffling firing rate across eight target locations 1000 times ($p<0.05$, permutation test). Since this procedure involves multiple comparisons, we corrected the p values by controlling for the false discovery rate (FDR).[67] Units with significant p-values either for target onset or saccade onset epochs were used for further analysis. Out of the 409 single units, we selected 216 neurons that showed an excitatory response inside the RF and had greater than 5 Hz firing rate either around target or saccade epoch (M1 = 122; M2 =139 neurons).

The ODR task further revealed the firing patterns of different LPFC neurons. We classified each unit that had an excitatory RF response into visual, visual-movement (VM) and movement neurons based on their firing patterns around target onset and saccadic eye movement. The delay period of the ODR task separated the visual and saccade related neuronal activity and allowed us to

Please cite this article in press as: Dubey et al., Top-down control of exogenous attentional selection is mediated by beta coherence in prefrontal cortex, Neuron (2023), https://doi.org/10.1016/j.neuron.2023.06.025

examine each neuron's firing patterns in response to target and saccade onset. Around target onset, visual and VM neurons showed an increase in firing activity and not movement neurons. Additionally, visual neurons reflected an increase in firing rate immediately after the target onset whereas VM neurons showed a delayed response (Figures 1 and S1A–S1C). Around saccade onset, VM and movement neurons showed an increase in firing activity and not visual neurons. Single unit responses at preferred target location were tested for selectivity around target onset and saccade onset through permutation testing. To classify between visual and VM neurons we compared each unit's baseline-subtracted firing rate around target onset epochs (0 to 100 ms and 75 to 200 ms, where 0 ms is target onset). To classify between movement and VM neurons we compared each unit's baseline-subtracted firing rate around saccade onset epoch (-50 to 70 ms where 0 ms is saccade onset). Units with significant p-values in target-onset (0 to 100 ms) epoch and not saccade-onset epoch were classified as visual neurons. Units with significant p-values in saccade-onset epoch and not target-onset epoch were classified as movement neurons. Units with significant p-values in both target-onset (75 to 200 ms) and saccade-onset epochs were classified as VM neurons. We further confirmed each unit's classification label by visual inspection. Out of 261 units, N=139 (M1=54, M2=85) were VM neurons, N=57 (M1=27, M2=30) were visual neurons and N=65 (M1=41, M2=24) were movement neurons.

QUANTIFICATION AND STATISTICAL ANALYSIS

LRS task selectivity

On the LRS task, the two targets were presented simultaneously. Therefore, on each trial, the location of both the targets with respect to a LPFC neuron's RF was identified. For further analysis, we pooled the data across two monkeys to increase the statistical power. For each neuron, we selected the subset of trials on which one target was inside the RF and the other was outside the RF. Trials on which both the targets were inside the RF or both the targets were outside the RF were removed from further analysis. We examined each neuron's selectivity to the LRS task based on the saccade response and the target properties. Trials on which saccade response was inside the RF were termed InRF trials and trials on which saccade response was outside the RF were termed OutRF trials. Figure 1F shows the population data of 139 VM neurons across 36864 InRF trials and 36455 OutRF trials. Similar to the ODR task, VM neurons responded significantly more on trials when the InRF target was selected compared to trials when the OutRF target was selected ($p=4.2 \times 10^{-3}$, Wilcoxon rank-sum test, epoch=50 to 200 ms). Firing rate increased soon after target onset and extended through the saccade. Movement neurons (N=65) also responded significantly more on the InRF (N=16450) trials compared to OutRF (N=16020) trials ($p=5.7 \times 10^{-5}$, Wilcoxon rank-sum test, epoch=150 to 250 ms). Visual neurons (N=57) however, showed comparable firing rates for InRF (N=14416) and OutRF (N=15651) trials (p=0.61, Wilcoxon rank-sum test, epoch=0 to 100 ms). The results were similar if different time-windows around the peak-firing rates were used ([56 304], [0 182], and [139 301] ms for VM, movement and visual neurons. These time-windows are determined based on half-firing rate, when the firing rates were half of the peak firing rate).

The InRF and OutRF trials were further subgrouped on the basis of attentional selection. Exo-InRF trials are exo-conflict trials on which Poor-Bright target was selected and target was in the RF, whereas Exo-OutRF trials are exo-conflict trials on which Poor-Bright target was selected and target was out of the RF. Similarly, Endo-InRF trials are endo-conflict trials on which Rich-Dim target was selected and the target was in the RF, whereas Endo-OutRF trials are endo-conflict trials on which Rich-Dim target was selected and the target was out of the RF. The subgrouping of InRF and OutRF trials based on attentional selection yielded the following number of trials for each subgroup. The trials were pooled across neurons in three cell-type (VM, visual and movement neurons) groups. VM neurons: Exo-InRF=5459, Exo-OutRF=5379, Endo-InRF=16842, and Endo-OutRF=16470 trials. Visual neurons: Exo-InRF=2308, Exo-OutRF=2567, Endo-InRF=644 and Endo-OutRF=6740 trials. Movement neurons: Exo-InRF=2548, Exo-OutRF=2540, Endo-InRF=7388 and Endo-OutRF=7230 trials.

Selection-time (ST) analysis

We estimated the onset of selectivity in firing rates as the time after target onset when firing rates differed significantly for InRF and OutRF selection. We did this by first calculating the firing rates using a 15 ms smoothing window and then computing the difference in InRF and OutRF firing rates for each neuron. We tested the mean difference in firing rate for each group (Figure 2E) against a null hypothesis that there is no difference in firing rates using a permutation test. A null distribution of firing rate differences was generated by shuffling the InRF and OutRF firing rates across neurons in each group 1000 times. We detected ST as the first time-point when InRF firing rates were significantly greater than OutRF rates ($p<0.01$, permutation test). Since this procedure involves multiple comparisons, we corrected the p values by controlling for the false discovery rate.

Spike-field coherence analysis

We estimated spike-field coherence (SFC) as a function of frequency using multitaper spectral estimation[68,69] with 10 Hz smoothing, and an estimation window spanning 200 ms before the target onset. The SFC was estimated between spiking and nearby LFP activity (within approx. 1.5 mm) to account for spiking activity bleeds into the LFP recording (Figures S3F and S3G). There was no spike amplitude for the broad-band recording on the LFP electrode when the activity was triggered on the spike times recorded on the other electrode.

The significance of SFC for each spike-field pair was tested against a null hypothesis that there was no SFC using a permutation test (1000 permutations, $p<0.05$). Null distribution for no SFC was generated by randomly permuting the order of trials for the spiking

data compared to the LFP data. Raw coherence values were converted to z-scores by subtracting the mean and then dividing by the standard deviation of the null distribution. We applied cluster correction to identify the significant clusters of p-values while accounting for multiple comparisons.[70] The significant cluster in beta (15-35 Hz) and gamma (40-70 Hz) frequency range was selected after performing a permutation test (1000 permutations, $p<0.05$). The coherent and not-coherent spike-field pairs in beta and gamma frequency ranges were identified based on the presence of a significant cluster in respective frequency bands. We identified 176 (M1=59, M2=117) coherent and 233 (M1=120, M2=113) not-coherent pairs in beta frequency range. A small number of spike-field pairs (10 out of 179 in M1 and 11 out of 230 in M2) were coherent in the gamma frequency range (Figure S3B).

Beta-amplitude analysis

At each recording site, we tested whether beta bursts are specifically present in the 200ms prior to target onset against the null hypothesis of activity at other times during the trial using a permutation test. Across the population, beta bursts were reliably present in ~96 % of recording sites in each animal (M1: 1108 out of 1152 sites; M2: 1299 out of 1344 sites; $p<0.05$, permutation test). We estimated amplitude of pre-target beta-burst for each trial at a single site, using multitaper spectral estimation.[68,69] We used 5 Hz smoothing, and an estimation window from 200 ms before target onset until target onset. The power values in beta (15-30 Hz) frequency range were converted to amplitude by taking square root. The logarithm transform of beta amplitude values were normalized with respect to mean across trials. We used these normalized beta-burst amplitude values for further analysis. Beta values varied trial-by-trial and observed a gaussian distribution at a given site (Figure 3B).

We examine the time-course of beta-burst related modulation in firing rates for exogenous and endogenous selection, by computing the beta values in six different 200 ms long time-windows (Figure 6). If otherwise mentioned beta related modulations were referred to beta values computed in 200 ms time-window before the target onset.

For a given site, we grouped the trials with the highest ~33% and lowest ~33% beta values to yield high-beta (HB) trials and low-beta (LB) trials. We calculated the SFC separately for HB and LB trials for coherent and not-coherent neurons.

Beta bursts and attentional selection

We compared the firing responses of VM neurons on high-beta and low-beta trials for exogenous and endogenous selection. We further subgrouped the exo/endo InRF and OutRF trials based on beta values to yield the following number of trials for each subgroup. VM neurons -high-beta: Exo-InRF=1818, Exo-OutRF=1801, Endo-InRF=5599, Endo-OutRF=5458 trials, VM neurons-low-beta: Exo-InRF=1808, Exo-OutRF=1815, Endo-InRF=5524, Endo-OutRF=5513 trials. Similarly, for visual neurons we yielded, high-beta: Exo-InRF=792, Exo-OutRF=866, Endo-InRF=2166, Endo-OutRF=2222 trials and low-beta: Exo-InRF=772, Exo-OutRF=867, Endo-InRF=2110, Endo-OutRF=2306 trials. And for movement neurons we yielded, high-beta: Exo-InRF=852, Exo-OutRF=863, Endo-InRF=2459, Endo-OutRF=2345 trials and low-beta: Exo-InRF=849, Exo-OutRF=843, Endo-InRF=2468, Endo-OutRF=2445 trials.

Permutation test

We tested the difference in firing rates on HB and LB trials for each group in Figures 4C, 5C, and 6C. We computed the difference in firing rates between LB and HB trials for each neuron and tested the mean difference across neurons against a null hypothesis that there is no difference in firing rates using a permutation test. A null distribution of firing rates difference was generated by shuffling the HB and LB firing rates across neurons in each group 1000 times ($p<0.01$, permutation test). Since this procedure involves multiple comparisons, we corrected the p values by controlling for the false discovery rate.

We tested the difference in RTs after stratifying trials according to beta value for endogenous-conflict and exogeneous-conflict trials as shown in Figure 7A. We performed this test separately for each monkey. For each group of trials, we computed the test statistic given by the maximum difference in RT (range = max RT - min RT) after stratifying trials by beta value. We then tested the hypothesis that the difference in RT across beta values differed for the specific group of exogenous or endogenous trials using a permutation test. A null distribution of the test statistic was generated by shuffling the trial labels within each group (exogenous-conflict and endogenous-conflict) separately. We then computed the RT for trials stratified by beta values as for the original data set. RT for each group was standardized to be mean 1 before permuting by dividing by the mean RT in each group. Beta values for each group were standardized to be mean zero for each group before permuting by subtracting the mean beta value in each group. We performed this permutation 1000 times and compared the maximum difference in RT for each permutation with the test statistic ($p<0.01$, permutation test). We used an analogous procedure to test for a significant difference in RTs after stratifying trials according to beta value for luminance-only and reward-only trials, as shown in Figure 7B. Since this procedure was performed once per monkey and group, it was not necessary to control for multiple comparisons.